

🔥 RITUAL: Random Image Transformations as a Universal Anti-hallucination Lever in Large Vision Language Models

Sangmin Woo* Jaehyuk Jang* Donguk Kim* Yubin Choi Changick Kim
KAIST

{smwoo95, jhyuk, kdu3613, choibinbin, changick}@kaist.ac.kr

Project: <https://sangminwoo.github.io/RITUAL/>

Abstract

Recent advancements in Large Vision Language Models (LVLMs) have revolutionized how machines understand and generate textual responses based on visual inputs, yet they often produce "hallucinatory" outputs that misinterpret visual information, posing challenges in reliability and trustworthiness. We propose 🔥 RITUAL, a simple decoding method that reduces hallucinations by leveraging randomly transformed images as complementary inputs during decoding, adjusting the output probability distribution without additional training or external models. Our key insight is that random transformations expose the model to diverse visual perspectives, enabling it to correct misinterpretations that lead to hallucinations. Specifically, when a model hallucinates based on the original image, the transformed images—altered in aspects such as orientation, scale, or color—provide alternative viewpoints that help recalibrate the model's predictions. By integrating the probability distributions from both the original and transformed images, RITUAL effectively reduces hallucinations. To further improve reliability and address potential instability from arbitrary transformations, we introduce RITUAL+, an extension that selects image transformations based on self-feedback from the LVLM. Instead of applying transformations randomly, RITUAL+ uses the LVLM to evaluate and choose transformations that are most beneficial for reducing hallucinations in a given context. This self-adaptive approach mitigates the potential negative impact of certain transformations on specific tasks, ensuring more consistent performance across different scenarios. Experiments demonstrate that RITUAL and RITUAL+ significantly reduces hallucinations across several object hallucination benchmarks.

1. Introduction

Large Vision-Language Models (LVLMs) [1, 8, 32, 33, 69] have emerged as a pivotal technology, enabling machines to

*Equal contribution

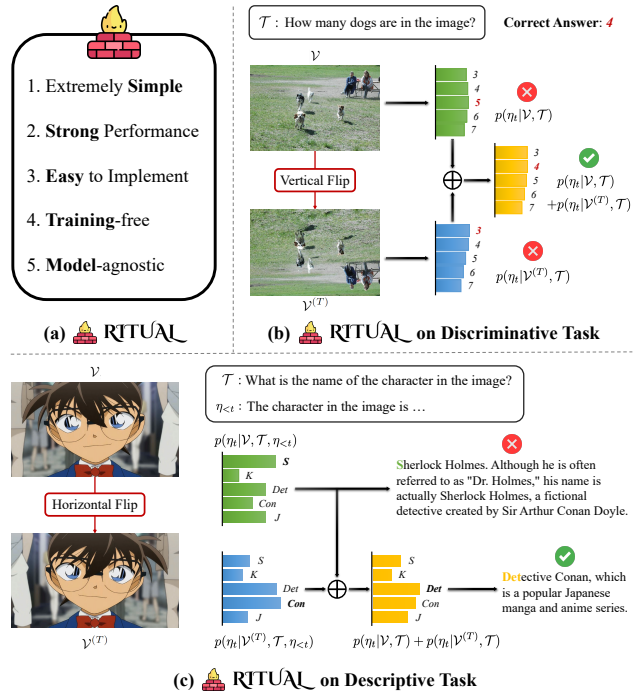



Figure 1. 🔥 RITUAL: A simple yet effective anti-hallucination approach for LVLMs. Our RITUAL method leverages basic image transformations (e.g., vertical and horizontal flips) to enhance LVLM accuracy without external models or training. By integrating transformed and original images, RITUAL significantly reduces hallucinations in both discriminative tasks and descriptive tasks. Using both versions together enables the model to refine predictions, reducing errors and boosting correct responses.

interpret complex visual scenes and generate contextually appropriate textual descriptions. These models integrate and process inputs from both visual and linguistic domains, offering unprecedented possibilities in applications ranging from video content creation [2] to assistive technologies [36, 47].

Despite these advancements, LVLMs still face a fundamental challenge: the tendency to produce "hallucinations" [18, 28, 53, 66]—outputs that are inconsistent with the actual content of the visual input. This gap in reliability and trustworthiness is particularly concerning for sensi-

tive applications such as medical diagnosis [34, 67], surveillance [16, 56], and autonomous driving [29].

Hallucinations in LVLMs often arise due to the model’s overreliance on certain visual cues or its inability to generalize effectively across diverse visual perspectives. Existing approaches to mitigate hallucinations often require complex training regimes [15, 20, 31, 35, 45, 50, 59, 61, 62, 68], sophisticated feedback mechanisms [21, 45, 59, 60], or reliance on auxiliary models [9, 26, 49, 57, 65], which can complicate deployment and scalability.

We present a simple, training-free approach termed  **RITUAL**, which leverages random image transformations to complement the original image and enhance models’ robustness (see Fig. 1). Our core insight is that by exposing the model to diverse visual transformations—such as changes in orientation, scale, and color—during decoding, it can better discern the true contents of the original image and reduce the likelihood of generating hallucinatory outputs. Specifically, **RITUAL** introduces these transformed images as complementary inputs during the decoding process, allowing the LVLM to adjust its output probability distribution by integrating alternative visual perspectives. **RITUAL** employs a dual-input strategy that integrates both the original and a randomly transformed image, and the final prediction is an ensemble of the individual predictions generated from both the original and augmented images. This simple yet effective approach does not require additional training or external models and is readily compatible with existing LVLMs.

To further enhance reliability, we propose **RITUAL+**, an adaptive extension of **RITUAL** that leverages self-feedback from the LVLM to guide the selection of transformations. Rather than applying random transformations indiscriminately, **RITUAL+** employs the LVLM itself to evaluate and choose the transformations that are most likely to mitigate hallucinations in a specific context. This self-adaptive mechanism mitigates the potential for detrimental transformations, which may inadvertently introduce instability in the model’s predictions, ensuring that our method performs consistently across a range of tasks and scenarios.

Our experiments evaluate **RITUAL** and **RITUAL+** across several benchmarks, including POPE [41], CHAIR [28], and both MME-Hallucination and MME-Fullset [13]. Despite its simplicity, our approach effectively reduces hallucination across these benchmarks, significantly enhancing the general capabilities of LVLMs. Moreover, **RITUAL** and **RITUAL+** consistently outperform existing contrastive decoding baselines [6, 12, 24] on all tested benchmarks, achieving superior performance with comparable latency.

2. Related Work

Hallucinations in LVLMs. LVLMs are susceptible to visual hallucinations, in which the generated text descriptions include objects or details entirely irrelevant from the given

image. A range of methods has been introduced to address the issue by additional training [15, 20, 31, 35, 45, 50, 59, 61, 62, 68]. While these approaches offer promise, they often face practical limitations due to their dependence on additional data and extensive training periods. In response to these limitations, training-free approaches have gained traction. These models aim to refine the model output by self-feedback correction [23, 59], providing additional knowledge using auxiliary models [9, 21, 49, 57, 65], and contrastive decoding [12, 24, 54, 64], which refines the model outputs by contrasting the conditional probability of textual responses given the original visual input versus a distorted visual input. Our work adopts a unique approach by applying random image transformations to complement the original image. This provides a wide range of visual contexts, aiming to mitigate hallucinatory visual explanations without the complexities of extra models, additional training, or data requirements.

Image augmentations for model robustness. Image augmentations [39, 44] have long been recognized as a crucial technique for improving model robustness, particularly in computer vision and multimodal tasks. By introducing variations in input data, augmentations help models generalize better to unseen scenarios, reduce overfitting, and improve performance in the presence of noise or ambiguous inputs. In the training phase, data augmentation techniques [7, 46], such as those used in SimCLR [4] and BYOL [14], enhance the diversity of training data by applying transformations like rotations, flips, and crops. This encourages the model to learn more generalizable features, improving performance on unseen data. At inference time, test-time augmentation (TTA) [38, 43, 63] further improves model robustness. TTA applies multiple transformations to the input image during testing, generating varied predictions which are then averaged or ensembled to produce a more reliable output. By exposing the model to diverse perspectives of the same input, TTA reduces sensitivity to noise and ambiguity, stabilizes predictions on difficult cases, and serves as a cost-effective ensembling method without requiring additional model training. Our approach builds on these concepts by using random image transformations during inference to provide a broader visual context, reducing hallucinations in vision-language models. By combining predictions from both the original and transformed images, our method enhances robustness.

3. Approach: **RITUAL**

We present a simple yet effective decoding method that is training-free and operates without the need for external models. An overview of our method is illustrated in Fig. 2.

3.1. LVLM Formulation

Vision-Language Alignment. LVLM takes a visual input and a textual query as inputs, where the visual input pro-

vides contextual visual information to assist the model in generating a relevant response to the textual query. Initially, a vision encoder (e.g., ViT [11], CLIP [40], etc.) processes raw images to extract visual features. These features are then projected into the language model’s input space using a vision-language alignment module (e.g., Q-Former [25], linear projection [33], etc.), resulting in a set of visual tokens, $\mathcal{V} = \{\nu_0, \nu_1, \dots, \nu_{N-1}\}$. Concurrently, the textual inputs are tokenized into $\mathcal{T} = \{\tau_N, \tau_{N+1}, \dots, \tau_{N+M-1}\}$. The visual and textual tokens are concatenated to form an input sequence of length $N + M$.

Model Forwarding. The LVLM, parametrized by θ , processes the concatenated sequence of visual and textual tokens. This process is formalized as:

$$\mathcal{H} = \text{LVLM}_\theta([\mathcal{V}, \mathcal{T}]), \quad (1)$$

where \mathcal{H} denotes the sequence of output hidden states from the final layer of LVLM. These hidden states \mathcal{H} are used to compute the logits (or probabilities) for predicting the next tokens.

Response Generation. The LVLM generates responses auto-regressively, employing a causal attention mask to ensure each subsequent token is predicted based solely on the preceding tokens. Each response token is generated by sampling from the following probability distribution:

$$\eta_t \sim p_\theta(\eta_t | \mathcal{V}, \mathcal{T}, \eta_{<t}). \quad (2)$$

where η_t denotes the response token being generated at timestep t , and $\eta_{<t}$ indicates the sequence of tokens generated up to timestep $(t - 1)$. This generative process is iteratively continued, appending each newly predicted token to the sequence, until the termination of the sequence. By default, standard multinomial sampling is used. Alternatively, decoding strategies such as Beam Search [55], Nucleus Sampling [17], or DoLa [6] can be employed.

3.2. Anti-hallucinating LVLMs with RITUAL

Visual hallucinations in LVLMs can occur during the decoding phase when tokens are selected based on erroneous probability distributions that do not align with the visual inputs. Our approach aims to mitigate these visual hallucinations with a simple yet effective modification to the input handling.

RITUAL first randomly apply common image transformations (e.g., Crop, Flip, Rotate, etc.) to the original visual input \mathcal{V} , This results in a transformed version of the visual input, $\mathcal{V}^{(T)}$.

$$\mathcal{V}^{(T)} = T(\mathcal{V}; \omega), \text{ where } \omega \in \Omega. \quad (3)$$

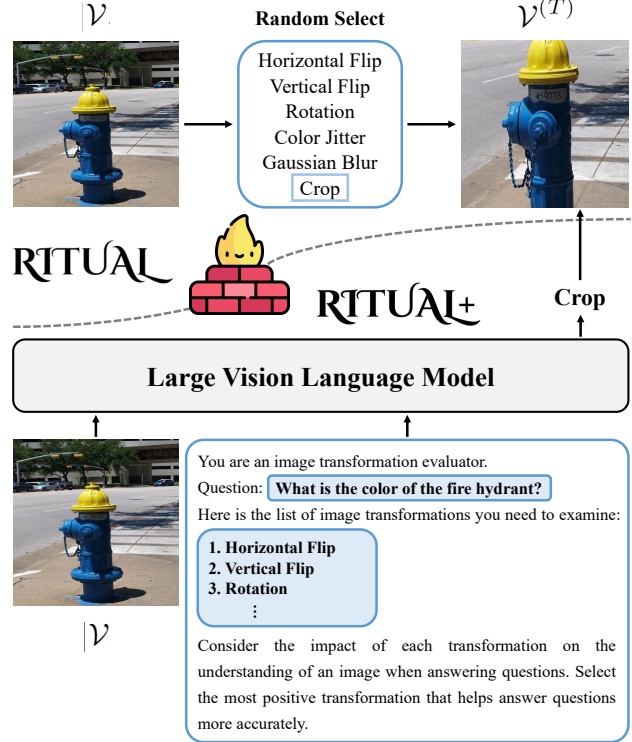


Figure 2. Overview of RITUAL and RITUAL+. In RITUAL, the original image \mathcal{V} undergoes random transformations, generating a transformed image $\mathcal{V}^{(T)}$. In RITUAL+, the model evaluates various potential transformations and selects the most beneficial one to improve answer accuracy within the given context, further refining reliability. These transformed images serve as complementary inputs, enabling the model to incorporate multiple visual perspectives to reduce hallucinations.

Here, T represents a specific transformation function selected randomly from a set of image transformations. The parameter ω represents the specific parameters of the transformation, drawn from a distribution Ω that governs the selection and nature of the transformation applied.

During the decoding phase, we utilize both the original and transformed images. The sampling equation in Eq. (2) is updated as follows:

$$\eta_t \sim p_\theta(\eta_t | \mathcal{V}, \mathcal{T}, \eta_{<t}) + \alpha p_\theta(\eta_t | \mathcal{V}^{(T)}, \mathcal{T}, \eta_{<t}). \quad (4)$$

Here, α is a balancing hyperparameter, adjusting the contribution of the transformed input relative to the original.

Image transformations. We employ a predefined set of image transformations to enhance model robustness, divided into geometric and appearance transformations. Geometric transformations, such as flipping, small random rotations, and cropping, simulate different viewing angles, orientations, and focus areas, enhancing the model’s ability to generalize across varied perspectives and object positioning. Appearance transformations, including color jitter and Gaussian

Table 1. **Impact of individual image transformations across various tasks on the MME-Hallucination benchmark [13].** Each transformation demonstrates varying degrees of effectiveness across different tasks, suggesting the need to carefully select transformations based on the specific image and task requirements.

Method		LLaVA 1.5 [33]			
		Existence	Count	Position	Color
<i>base</i>		190.00	140.00	120.00	160.00
<i>Transformation</i>	+ Color Jitter	190.00	130.00 ↓	126.67 ↑	143.33 ↓
	+ Crop	190.00	123.33 ↓	128.33 ↑	170.00 ↑
	+ Gaussian Blur	195.00 ↑	146.67 ↑	123.33 ↑	170.00 ↑
	+ Horizontal Flip	195.00 ↑	158.33 ↑	111.67 ↓	165.00 ↑
	+ Rotation	190.00	141.67 ↑	116.67 ↓	165.00 ↑
	+ Vertical Flip	190.00	140.00	115.00 ↓	160.00

blur, adjust brightness, contrast, and saturation to account for lighting variations and sensor noise, increasing resilience to image imperfections. Together, these transformations introduce meaningful variations that better prepare the model for real-world image scenarios, improving its flexibility and performance.

3.3. Adaptive Transformation Selection: $\text{RTU}\mathcal{A}\mathcal{L}_+$

Despite the diverse views offered by random transformations by $\text{RTU}\mathcal{A}\mathcal{L}$, the effectiveness of each transformation varies depending on the image, query, and task. Table 1 summarizes the performance of $\text{RTU}\mathcal{A}\mathcal{L}$ when employing individual augmentations. Gaussian Blur and Horizontal Flip improve counting and existence tasks, transformations like Crop degrade counting accuracy, and flips or rotations disrupt positional understanding. Color Jitter also negatively affect color-related tasks, while Gaussian Blur and Crop enhance them.

To further enhance reliability and address these inconsistencies, we propose $\text{RTU}\mathcal{A}\mathcal{L}_+$, a self-adaptive extension of $\text{RTU}\mathcal{A}\mathcal{L}$. $\text{RTU}\mathcal{A}\mathcal{L}_+$ leverages LVLm self-feedback to evaluate the impact of each transformation within the specific context of the image and query. Instead of relying on random augmentation, it selects transformations that are most effective in minimizing hallucinations and enhancing task-specific performance. By dynamically tailoring augmentations to the requirements of the task, $\text{RTU}\mathcal{A}\mathcal{L}_+$ mitigates negative effects, such as the disruption of positional understanding or feature distortions, and ensures more robust and consistent results across diverse scenarios.¹

4. Experiments

4.1. Evaluation Setup

Throughout our experiments, we set hyperparameter configuration at $\alpha = 3$. For random image transformation, we use flip (horizontal & Vertical), rotate, color jitter, Gaussian blur, and crop. In all experimental tables, *base* refers

¹More details about $\text{RTU}\mathcal{A}\mathcal{L}_+$ are in Appendix.

to standard decoding, where the token is directly sampled from the softmax distribution. To encourage output diversity and avoid deterministic responses, we sample from a multinomial distribution rather than simply selecting the most probable output using argmax .²

LVLms. We integrate $\text{RTU}\mathcal{A}\mathcal{L}$ with three state-of-the-art LVLms: **LLaVA-1.5** [33], **InstructBLIP** [8], and **mPLUG-Owl2** [58]. Both LLaVA-1.5 and InstructBLIP use Vicuna 7B [5] for language decoding. LLaVA-1.5 utilizes two-layer MLP to align image and text modalities and InstructBLIP employs the Q-Former [25] with a fixed number of tokens (e.g., 32) to bridge visual and textual features efficiently. mPLUG-Owl2, built on LLaMA 7B [48], combines a vision encoder with learnable queries and a modality-adaptive module to facilitate a shared semantic space between visual and textual modalities. Note that $\text{RTU}\mathcal{A}\mathcal{L}$ is model-agnostic, and its adaptability extends beyond these LVLms.

Baselines. Our method aims to reduce hallucinations in LVLms by modifying model’s decoding process without relying on external models, costly self-feedback mechanisms, or additional training. To align with these criteria, we select baseline methods that meet these requirements. Recent contrastive decoding methods fit well within this scope, and we establish two primary baselines: **VCD** [24] and **M3ID** [12]. Both VCD and M3ID aim to mitigate object hallucinations by increasing the influence of the reference image over the language prior. This is achieved by contrasting output distributions derived from both original and distorted visual inputs. We also include **DoLa** [6] as a baseline, which employs a novel decoding strategy that contrasts logits from earlier and later layers of the transformer architecture. This amplifies factual knowledge stored in the upper layers while suppressing linguistic patterns from the lower layers that may lead to hallucinations. Additionally, we report results from **OPERA** [18], which mitigates hallucinations in LVLms via an over-trust penalty and retrospection allocation. In contrast to all other methods, OPERA uses beam search during response generation, contributing to its higher performance. We include it for comparison purposes due to its demonstrated effectiveness in reducing hallucinations. All methods were reimplemented in our evaluation setup to ensure a fair comparison.

Benchmarks. (1) **POPE** [28] frames hallucination assessment as a binary classification task using yes/no questions about object presence (e.g., "Is there a dog in the image?"). It evaluates 500 MS-COCO images with questions based on actual objects or nonexistent objects. The benchmark contains three subsets (random, popular, and adversarial), addressing object prevalence and co-occurrences. (2) **MME** [13] is a comprehensive

²Further implementation & experimental details are in Appendix.

Table 2. **Results on POPE [28] benchmark.** RITUAL consistently outperforms the contrastive decoding baselines: VCD [24], M3ID [12], and DoLa [6]. RITUAL \pm employs standard decoding but achieves performance comparable to OPERA [18], which uses beam search. *Note: All baseline methods were reimplemented within our evaluation setup for fair comparison.*

Setup	Method	LLaVA 1.5 [33]				InstructBLIP [8]				mPLUG-Owl2 [58]				
		Acc. \uparrow	Prec. \uparrow	Rec. \uparrow	F1 \uparrow	Acc. \uparrow	Prec. \uparrow	Rec. \uparrow	F1 \uparrow	Acc. \uparrow	Prec. \uparrow	Rec. \uparrow	F1 \uparrow	
MS-COCO [30]	Random	base	84.13	82.86	86.07	84.43	82.80	82.24	83.67	82.95	81.00	75.27	92.33	82.93
		VCD	85.37	83.14	88.73	85.84	83.93	84.42	82.67	83.73	81.53	76.40	91.27	83.17
		M3ID	86.00	85.11	87.27	86.18	84.37	84.62	84.00	84.31	80.90	75.29	92.00	82.81
		DoLa	85.97	85.10	87.20	86.14	84.00	82.86	85.73	84.27	81.20	75.97	91.27	82.92
		RITUAL	88.87	89.23	88.40	88.81	88.83	90.48	86.80	88.60	84.83	80.40	92.13	85.87
		RITUAL \pm	89.17	88.89	89.53	89.21	88.67	90.28	86.67	88.44	85.57	81.18	92.60	86.52
	OPERA (Beam)	89.37	92.03	86.20	89.02	89.17	95.51	82.20	88.36	89.27	89.48	89.00	89.24	
	Popular	base	80.87	78.23	85.53	81.72	75.80	72.74	82.53	77.33	76.27	69.96	92.07	79.50
		VCD	81.10	77.78	87.07	82.16	77.73	75.43	82.27	78.70	75.70	69.88	90.33	78.80
		M3ID	82.83	79.62	88.27	83.72	77.30	74.10	83.93	78.71	76.50	70.23	92.00	79.65
		DoLa	82.93	79.76	88.27	83.80	77.37	73.50	85.60	79.09	76.67	70.58	91.47	79.67
		RITUAL	85.83	84.17	88.27	86.17	81.97	78.90	87.27	82.87	80.43	74.64	92.20	82.49
		RITUAL \pm	86.65	85.35	88.67	86.98	82.63	79.65	87.67	83.47	80.83	75.62	91.00	82.60
	OPERA (Beam)	86.20	85.17	87.67	86.40	84.07	85.39	82.20	83.76	84.13	81.11	89.00	84.87	
	Adversarial	base	76.23	71.75	86.53	78.45	75.40	71.60	84.20	77.39	73.20	66.88	91.93	77.43
		VCD	75.60	70.78	87.20	78.14	76.80	73.62	83.53	78.26	73.23	67.26	90.53	77.18
		M3ID	77.70	73.23	87.33	79.66	76.03	72.48	83.93	77.79	72.57	66.28	91.87	77.00
		DoLa	77.17	72.30	88.07	79.41	74.30	69.95	85.20	76.83	72.37	66.29	91.00	76.71
RITUAL		78.80	74.43	87.73	80.54	78.73	74.57	87.20	80.39	75.23	68.88	92.07	78.80	
RITUAL \pm		79.37	74.62	89.00	81.18	78.63	74.70	86.60	80.21	75.57	69.24	92.00	79.02	
OPERA (Beam)	81.07	77.44	87.67	82.24	81.83	81.60	82.20	81.90	80.00	75.42	89.00	81.65		
A-OKVQA [42]	Random	base	81.73	76.53	91.53	83.36	81.13	78.03	86.67	82.12	78.13	70.87	95.53	81.37
		VCD	81.83	75.74	93.67	83.76	82.00	79.38	86.47	82.77	77.70	70.42	95.53	81.07
		M3ID	83.57	77.86	93.80	85.09	82.33	77.81	90.47	83.66	78.23	70.73	96.33	81.57
		DoLa	83.23	77.47	93.73	84.83	82.17	78.17	89.27	83.35	77.67	70.38	95.53	81.05
		RITUAL	85.17	79.79	94.20	86.40	87.13	83.92	91.87	87.71	80.20	73.02	95.80	82.87
		RITUAL \pm	85.43	80.15	94.20	86.81	87.40	84.42	91.73	87.92	80.37	73.35	95.40	82.93
	OPERA (Beam)	86.80	82.90	92.73	87.54	89.97	90.75	89.00	89.87	86.57	82.17	93.40	87.43	
	Popular	base	76.67	70.51	91.67	79.71	75.67	70.97	86.87	78.12	71.27	64.43	94.93	76.77
		VCD	74.70	68.12	92.87	78.59	76.50	71.69	87.60	78.85	71.07	64.21	95.20	76.69
		M3ID	76.80	70.20	93.13	80.06	75.60	70.40	88.33	78.36	69.57	62.80	96.00	75.93
		DoLa	76.47	69.79	93.33	79.86	76.93	71.15	90.60	79.71	71.10	64.22	95.27	76.72
		RITUAL	78.83	71.99	94.40	81.68	78.73	72.83	91.67	81.17	74.20	66.96	95.53	78.74
		RITUAL \pm	79.13	72.30	94.47	81.91	79.00	72.92	92.27	81.46	74.37	66.93	96.33	78.98
	OPERA (Beam)	79.60	73.44	92.73	81.97	82.60	78.90	89.00	83.65	80.90	74.72	93.40	83.02	
	Adversarial	base	67.40	61.78	91.27	73.68	68.00	63.08	86.80	73.06	64.83	59.15	95.87	73.16
		VCD	67.43	61.48	93.33	74.13	70.67	65.24	88.47	75.10	66.43	60.39	95.53	74.00
		M3ID	68.10	61.99	93.60	74.58	69.57	64.21	88.40	74.39	65.13	59.33	96.27	73.41
		DoLa	68.03	62.02	93.07	74.43	68.50	62.94	90.00	74.07	65.73	59.91	95.13	73.52
RITUAL		68.57	62.26	94.27	74.99	70.27	64.15	91.87	75.55	65.93	59.99	95.67	73.74	
RITUAL \pm		68.80	62.51	94.47	75.23	70.97	64.74	92.07	76.03	66.20	60.12	96.27	74.01	
OPERA (Beam)	70.00	63.75	92.73	75.56	74.53	69.03	89.00	77.75	71.17	64.65	93.40	76.41		
GQA [19]	Random	base	81.23	75.42	92.67	83.16	79.93	76.73	85.93	81.07	80.00	74.04	92.40	82.21
		VCD	81.50	74.78	95.07	83.71	81.83	79.03	86.67	82.67	81.60	77.56	88.93	82.86
		M3ID	82.83	76.64	94.47	84.62	80.57	76.77	87.67	81.85	80.93	74.95	92.93	82.98
		DoLa	83.70	77.70	94.53	85.29	81.57	77.90	88.13	82.70	78.67	73.19	90.47	80.92
		RITUAL	86.10	80.30	95.67	87.31	84.87	82.52	88.47	85.39	82.10	76.10	93.60	83.95
		RITUAL \pm	86.77	81.00	96.40	88.03	85.43	83.20	88.80	85.91	82.60	76.66	93.73	84.34
	OPERA (Beam)	87.07	82.25	94.53	87.97	87.70	90.02	84.80	87.33	86.27	85.65	87.13	86.38	
	Popular	base	72.50	65.85	93.47	77.27	72.73	68.14	85.40	75.80	71.53	64.94	93.60	76.68
		VCD	71.57	64.72	94.80	76.93	73.67	68.82	86.53	76.67	71.40	65.77	89.27	75.74
		M3ID	72.83	66.04	94.00	77.58	74.57	69.45	87.73	77.53	71.50	65.06	92.87	76.52
		DoLa	74.03	66.85	95.33	78.59	73.70	68.58	87.47	76.88	71.03	65.23	90.07	75.67
		RITUAL	74.80	67.50	95.67	79.15	74.50	69.17	88.40	77.61	73.47	66.60	94.13	78.01
		RITUAL \pm	75.47	68.32	96.20	79.90	76.10	70.49	89.80	78.98	73.93	66.95	94.53	78.39
	OPERA (Beam)	75.50	68.47	94.53	79.42	78.77	75.67	84.80	79.97	76.60	71.97	87.13	78.83	
	Adversarial	base	67.63	61.68	93.13	74.21	69.57	64.80	85.67	73.79	68.73	62.60	93.07	74.85
		VCD	67.47	61.38	94.20	74.33	69.43	64.76	85.27	73.61	71.67	65.98	89.47	75.95
		M3ID	68.13	61.88	94.47	74.78	68.90	64.06	86.13	73.47	68.23	62.29	92.40	74.42
		DoLa	68.73	62.34	94.67	75.17	69.70	64.28	88.67	74.53	69.50	63.51	91.67	75.03
RITUAL		68.23	61.75	95.80	75.10	70.17	64.76	88.47	74.78	68.30	62.15	93.60	74.70	
RITUAL \pm		69.17	62.42	96.33	75.75	70.60	65.04	89.07	75.18	69.63	63.19	94.07	75.60	
OPERA (Beam)	70.00	63.42	94.53	75.91	74.40	70.20	84.80	76.81	73.33	68.29	87.13	76.57		

Table 3. **Results on MME-Hallucination [13]**. RITUAL effectively mitigates hallucinations at both the object and attribute levels, outperforming contrastive decoding methods in Total Score. RITUAL_+ further enhances performance by adaptively selecting appropriate augmentations, leading to improved mitigation of hallucinations.

Model	Method	Object-level		Attribute-level		Total Score
		Existence \uparrow	Count \uparrow	Position \uparrow	Color \uparrow	
LLaVA1.5	<i>base</i>	173.75(± 4.79)	121.67(± 12.47)	117.92(± 3.69)	149.17(± 7.51)	562.50(± 3.96)
	VCD	178.75(± 2.50)	126.25(± 10.40)	120.00(± 4.08)	150.83(± 11.01)	575.84(± 9.67)
	M3ID	177.50(± 6.45)	124.17(± 10.93)	120.00(± 7.07)	152.92(± 5.67)	574.59(± 9.75)
	DoLa	174.58(± 5.34)	122.09(± 11.73)	122.09(± 2.10)	149.17(± 4.19)	567.92(± 13.63)
	RITUAL	187.50(± 2.89)	139.58(± 7.62)	125.00(± 10.27)	164.17(± 6.87)	616.25(± 20.38)
	RITUAL_+	188.89(± 6.74)	145.55(± 2.55)	110.00(± 21.86)	173.89(± 10.58)	618.33(± 28.04)
InstructBLIP	<i>base</i>	160.42(± 5.16)	79.17(± 8.22)	79.58(± 8.54)	130.42(± 17.34)	449.58(± 24.09)
	VCD	158.75(± 7.25)	90.75(± 3.11)	70.00(± 15.81)	132.50(± 18.78)	452.00(± 31.57)
	M3ID	158.33(± 5.44)	94.58(± 9.85)	72.50(± 17.03)	128.33(± 14.72)	453.75(± 26.82)
	DoLa	162.08(± 5.34)	82.50(± 6.16)	78.75(± 8.96)	135.42(± 10.49)	458.75(± 11.25)
	RITUAL	182.50(± 6.45)	74.58(± 5.99)	67.08(± 10.31)	139.17(± 0.96)	463.33(± 12.40)
	RITUAL_+	187.22(± 5.09)	88.89(± 13.47)	72.22(± 7.52)	148.33(± 10.93)	496.67(± 4.41)
mPLUG-Owl2	<i>base</i>	174.58(± 4.17)	155.42(± 10.03)	81.67(± 14.72)	141.25(± 13.29)	552.92(± 9.94)
	VCD	170.00(± 0.00)	138.75(± 6.44)	81.25(± 12.65)	138.75(± 5.51)	528.75(± 12.50)
	M3ID	176.25(± 4.79)	157.92(± 9.75)	81.67(± 14.72)	142.50(± 12.51)	558.33(± 10.28)
	DoLa	175.00(± 5.77)	151.67(± 5.61)	82.09(± 14.17)	139.58(± 5.51)	548.33(± 8.92)
	RITUAL	185.00(± 4.08)	159.58(± 13.57)	77.50(± 9.57)	160.42(± 4.59)	582.5(± 21.71)
	RITUAL_+	189.44(± 5.09)	159.45(± 5.36)	83.33(± 20.48)	162.22(± 8.55)	594.45(± 39.48)

LVLm benchmark assessing 14 subtasks, including object hallucination through tasks like object existence, count, position, and color. These tasks are framed as binary yes/no questions. (3) **CHAIR** [41] evaluates the proportion of words in captions that correspond to actual objects in an image, using ground-truth captions and object annotations. It has two variants: (i) per-sentence (CHAIR_S) is defined as $|\{\text{sentences with hallucinated objects}\}|/|\{\text{all sentences}\}|$. (ii) per-instance (CHAIR_I) is defined as $|\{\text{hallucinated objects}\}|/|\{\text{all objects mentioned}\}|$. We randomly select 500 images from the COCO [30] validation set and conduct image captioning with the prompt "Please describe this image in detail".

4.2. Results

Results on POPE. Table 2 compares various decoding-based hallucination mitigation methods on the POPE benchmark [28], reporting results from the same sampling-based decoding approach (sampling from a multinomial distribution). The results demonstrate that RITUAL consistently outperforms standard decoding (*base*) and contrastive decoding baselines [6, 12, 24], across all datasets (MS-COCO [30], A-OKVQA [42], and GQA [19]), setups (random, popular, and adversarial), and evaluation metrics, demonstrating its robustness in mitigating object hallucinations. Moreover, RITUAL_+ achieves performance comparable to the beam search-based method OPERA [18], despite its simpler design. This highlights the effectiveness of incorporating visual context from multiple perspectives.

Table 4. **Results on CHAIR [41]**. RITUAL and RITUAL_+ significantly reduce object hallucinations in caption generation compared to VCD, M3ID, and DoLa. The number of *max new tokens* is set to 64.

Method	$\text{CHAIR}_S \downarrow$	$\text{CHAIR}_I \downarrow$	
LLaVA1.5	<i>base</i>	26.2	9.3
	VCD	22.4	7.6
	M3ID	23.0	6.8
	DoLa	23.2	7.8
	RITUAL	20.6	6.9
	RITUAL_+	19.6	6.8
OPERA (beam)	23.0	7.5	
InstructBLIP	<i>base</i>	28.6	10.3
	VCD	27.2	9.1
	M3ID	31.8	10.4
	DoLa	36.6	12.5
	RITUAL	26.0	8.8
	RITUAL_+	24.2	8.0
OPERA (beam)	25.6	8.3	
mPLUG-Owl2	<i>base</i>	25.8	8.4
	VCD	24.0	7.8
	M3ID	22.8	7.3
	DoLa	26.2	8.5
	RITUAL	19.2	6.4
	RITUAL_+	18.0	5.5
OPERA (beam)	18.2	5.5	

Results on MME-Hallucination. In Table 3, we compare the results on the MME-hallucination benchmark [13] to assess the model’s effectiveness in reducing various types of hallucinations. When combined with LLaVA-1.5 [33], our approach consistently outperforms all counterparts across both object-level (Existence and Count) and attribute-level (Position and Color) evaluations. With InstructBLIP [8], while other methods show slight advantages in specific metrics like Count and Position, our method still surpasses the baseline and other contrastive decoding methods in overall Total Score. Some reductions in performance on Count and Position tasks can be attributed to certain transformations: for example, cropping can reduce visible object quantity, impacting the Count score, and flipping can alter spatial relationships, affecting Position score. RITUAL_+ addresses these limitations by adaptively selecting the most suitable transformations based on self-feedback, thereby overcoming challenges associated with individual transformations and improving performance. With mPLUG-Owl2, our method demonstrates strong performance as well, particularly excelling in Existence and Color tasks.

Results on CHAIR. To evaluate hallucinations in generative tasks, we use the CHAIR benchmark, which compares objects in the image with objects in the generated text to measure hallucination levels. For a fair comparison, we set the maximum number of new tokens to 64 across all methods. As shown in Table 4, RITUAL consistently outperforms both the baseline and prior contrastive decoding approaches. Specifically, with LLaVA 1.5, RITUAL achieves CHAIR_S

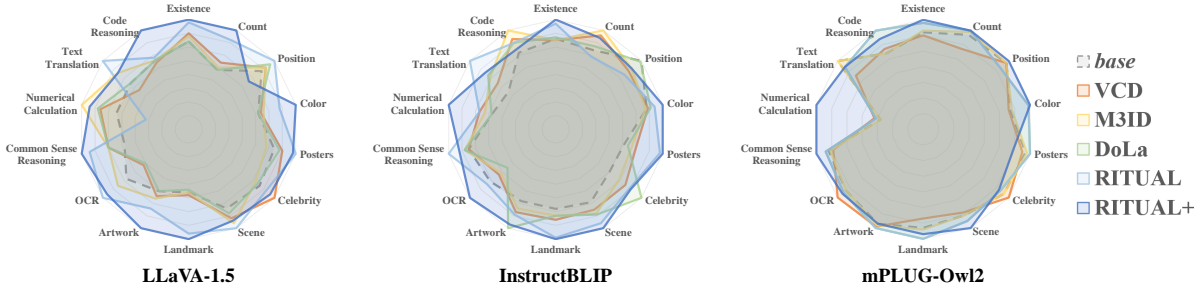


Figure 3. **Comparison on MME-Fullset [13].** RITUAL significantly enhances the general vision-language capabilities of LVLMs across wide range of tasks. When equipped with RITUAL , LLaVA-1.5 [33] achieves top performance in 12 of the 14 categories, while InstructBLIP [8] leads in 8 categories and mPLUG-Owl2 [58] ranks highest in 9 categories. Detailed results are in Appendix.

and CHAIR_I scores of 20.6 and 6.9, respectively, showing a substantial improvement over the baseline scores of 26.2 and 9.3. Although M3ID slightly outperforms RITUAL on CHAIR_I , RITUAL delivers comparable results while significantly excelling in CHAIR_S . For InstructBLIP, RITUAL achieves the best results, with CHAIR_S and CHAIR_I scores of 26.0 and 8.8, marking a major advancement over the baseline scores of 28.6 and 10.3. Similarly, with mPLUG-Owl2, RITUAL records CHAIR_S and CHAIR_I scores of 19.2 and 6.4, outperforming the baseline scores of 25.8 and 8.4 by a large margin. $\text{RITUAL}+$ further enhances these results, demonstrating the value of adaptive transformation selection. This adaptive approach not only benefits discriminative tasks but also proves effective for descriptive tasks that require a comprehensive understanding of the image content.

Results on MME-Fullset. The MME-Fullset [13] serves as a comprehensive benchmark for assessing the general vision-language capabilities of LVLMs beyond hallucination reduction, covering 14 diverse categories and use cases. As depicted in Fig. 3, we evaluate the impact of different decoding methods on LVLM performance across these categories. Across all tested LVLMs, RITUAL and $\text{RITUAL}+$ consistently achieves the highest scores across most tasks, demonstrating its effectiveness in enhancing vision-language comprehension beyond hallucination mitigation. By enriching the model’s understanding with diverse visual contexts, RITUAL provides balanced performance gains across a wide range of tasks, establishing itself as a robust and flexible method for improving LVLM performance. $\text{RITUAL}+$ further enhances these results, showing that adaptive transformation selection improves performance even on more general tasks, confirming the benefit of tailored augmentation for varied use cases. However, despite the additional visual information provided, some tasks still exhibit slightly lower performance due to inherent challenges within LVLMs, such as statistical biases and language priors.

4.3. Analysis

Textual Quality. Since previous methods and RITUAL modify the logits from the standard decoding strategy, there may be concerns about potentially compromising the quality of

Table 5. **GPT4-aided text quality evaluation.** Scores ranging from 1 to 10.

Method	LLaVA1.5	
	Grammar \uparrow	Fluency \uparrow
<i>base</i>	9.804	9.432
VCD	9.802	9.352
M3ID	9.832	9.344
DoLa	9.814	9.320
RITUAL	9.844	9.398
$\text{RITUAL}+$	9.850	9.421
OPERA (beam)	9.828	9.308

Table 6. **Comparison of performance and latency on POPE COCO random setup.**

Method	LLaVA1.5		
	Acc. \uparrow	F1 \uparrow	Latency (ms/token)
<i>base</i>	84.13	84.43	21.96
VCD	85.37	85.84	43.33
M3ID	86.00	86.18	40.07
DoLa	85.97	86.14	28.70
RITUAL	88.87	88.81	43.37
$\text{RITUAL}+$	89.17	89.21	69.27
OPERA (beam)	89.37	89.02	308.48

the generated text. Therefore, we employed GPT-4-Turbo to assess the grammar and fluency of generated text from 500 samples of the CHAIR benchmark [41] using the InstructBLIP [8]. As shown in Tab. 5, our decoding method demonstrates text generation quality that is comparable to or exceeds that of the previous work in terms of grammar and fluency. The results highlight the robustness and effectiveness of our method in generating grammatically correct and fluent text while also improving hallucination mitigation without compromising overall text generation quality.

Latency. Contrastive decoding methods like VCD [24] and M3ID [12], as well as RITUAL , require performing the forward process twice to compare two probability distributions, doubling resource consumption. Table 6 details the performance and speed comparison. In our experiments, DoLa [6] has minimal overhead compared to normal decoding, with only a $1.3\times$ increase in latency. DoLa is faster than RITUAL , but RITUAL shows better performance. Despite implementation differences such as beam search, OPERA [18] achieves slightly higher accuracy than RITUAL , but our method is significantly faster than OPERA. There are trade-offs among the methods, but RITUAL offers clear advantages. It is conceptually and implementation-wise simple, applicable to various methods, and delivers a favorable speed and performance trade-off. Also, it can be complementarily used with other contrastive decoding methods.

Ablation of the number of augmented images. To investigate whether increased exposure to diverse visual scenarios

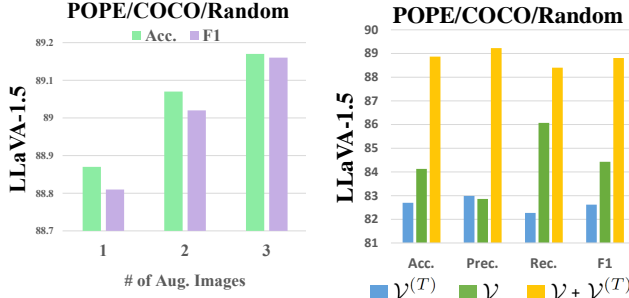


Figure 4. **Impact of the number of augmented images in RITUAL.**

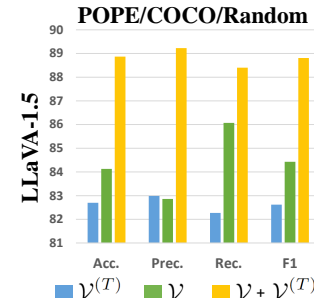


Figure 5. **Impact of combining original and transformed images.**

allows the model to better understand images and produce more robust responses, we conducted an ablation study by varying the number of augmented images in RITUAL. As shown in Fig. 4, the performance slightly improves as more augmented images are used. This improvement can be attributed to the richer visual context provided by the additional augmentations. However, using multiple augmented images also introduces a trade-off, as it increases latency due to the additional computational load.³

Original vs. Transformed vs. Combined Images. As shown in Fig. 5, the model’s performance declines when using only randomly transformed images ($\mathcal{V}^{(T)}$) as input compared to using the original images (\mathcal{V}). This drop in performance can likely be attributed to the introduction of visual artifacts and loss of essential cues, which disrupt the model’s contextual understanding. In contrast, using both the original and transformed images together ($\mathcal{V} + \mathcal{V}^{(T)}$) significantly enhances the model’s performance. This combined approach offers the model a richer, multiview representation, allowing it to leverage complementary perspectives from each view. As a result, the model achieves better generalization, reduces hallucinated responses, and improves the likelihood of producing correct answers across various tasks.

Compatibility with contrastive decoding methods.

As shown in Table 7, combining RITUAL with contrastive decoding methods like VCD and M3ID yields additional performance gains, underscoring the compatibility and complementary strengths of these approaches. While contrastive decoding helps reduce inherent language biases, RITUAL broadens the model’s visual perception by exposing it to diverse transformations and perspectives. This synergy effectively mitigates object hallucinations, leading to notable improvements in accuracy and F1 scores, demonstrating the potential of integrating diverse decoding strategies to enhance LLM reliability and

³Detailed results are in Appendix.

Table 7. **Compatibility w/ contrastive decoding.**

Method	LLaVA 1.5	
	Acc. \uparrow	F1 \uparrow
RITUAL	88.87	88.81
+ VCD	89.07	88.81
+ M3ID	89.00	88.88

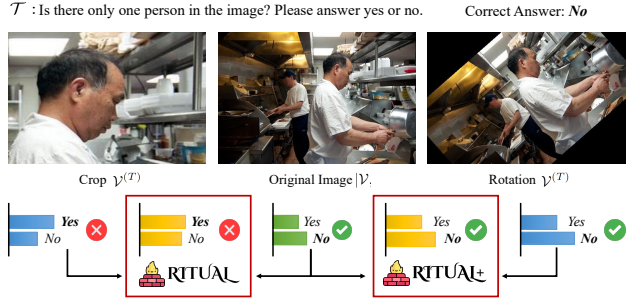


Figure 6. **Case study: RITUAL vs. RITUAL+.** RITUAL’s random transformations can miss key details like a person in the image, while RITUAL+ adaptively selects certain transformation in context (e.g., rotation) to yield correct answers, accurately identifying multiple people in the images.

comprehension.⁴

Case study. In Fig. 6, we compare RITUAL and RITUAL+ in handling a query "Is there only one person in the image?". RITUAL, which applies transformations randomly, may occasionally lead to detrimental choices. For example, performance may be impacted by the cropping area; in some cases, random cropping may inadvertently cut out important parts of the image, such as a person, resulting in poor outcomes. In contrast, RITUAL+ adapts to the query and image context, selecting transformations more strategically. In this case, RITUAL+ chooses rotation to interpret the image from a different angle, successfully identifying details that RITUAL missed, leading to a correct response.

5. Conclusion

We presented RITUAL, a simple decoding method that reduces hallucinations in LLMs by incorporating randomly transformed images as complementary inputs. To further enhance stability, RITUAL+ adaptively selects transformations based on self-feedback, ensuring consistent performance across tasks. Experiments show that both RITUAL and RITUAL+ outperform existing contrastive decoding methods on hallucination benchmarks and improve general vision-language understanding. Our approach is training-free, model-agnostic, easy-to-implement, and requires no external models, yet it delivers strong performance. This makes it a robust solution for enhancing LLM accuracy and trustworthiness across diverse applications.

Limitations. Like other contrastive decoding methods [6, 12, 24], RITUAL requires two forward passes, nearly doubling the latency compared to standard decoding. RITUAL+, which involves additional self-feedback for adaptive transformation selection, requires three passes, resulting in approximately triple the latency. This introduces a trade-off between improved hallucination mitigation and increased latency, which may impact usability in time-sensitive applications.

⁴Full results are in Appendix.

References

- [1] Jinze Bai, Shuai Bai, Shusheng Yang, Shijie Wang, Sinan Tan, Peng Wang, Junyang Lin, Chang Zhou, and Jingren Zhou. Qwen-vl: A versatile vision-language model for understanding, localization, text reading, and beyond. 2023. [1](#)
- [2] Tim Brooks, Bill Peebles, Connor Holmes, Will DePue, Yufei Guo, Li Jing, David Schnurr, Joe Taylor, Troy Luhman, Eric Luhman, Clarence Ng, Ricky Wang, and Aditya Ramesh. Video generation models as world simulators. 2024. [1](#)
- [3] Keqin Chen, Zhao Zhang, Weili Zeng, Richong Zhang, Feng Zhu, and Rui Zhao. Shikra: Unleashing multimodal llm’s referential dialogue magic. *arXiv preprint arXiv:2306.15195*, 2023. [12](#)
- [4] Ting Chen, Simon Kornblith, Mohammad Norouzi, and Geoffrey Hinton. A simple framework for contrastive learning of visual representations. In *International conference on machine learning*, pages 1597–1607. PMLR, 2020. [2](#), [18](#)
- [5] Wei-Lin Chiang, Zhuohan Li, Zi Lin, Ying Sheng, Zhanghao Wu, Hao Zhang, Lianmin Zheng, Siyuan Zhuang, Yonghao Zhuang, Joseph E Gonzalez, et al. Vicuna: An open-source chatbot impressing gpt-4 with 90%* chatgpt quality. See <https://vicuna.lmsys.org> (accessed 14 April 2023), 2(3):6, 2023. [4](#)
- [6] Yung-Sung Chuang, Yujia Xie, Hongyin Luo, Yoon Kim, James Glass, and Pengcheng He. Dola: Decoding by contrasting layers improves factuality in large language models. *arXiv preprint arXiv:2309.03883*, 2023. [2](#), [3](#), [4](#), [5](#), [6](#), [7](#), [8](#), [14](#), [16](#)
- [7] Ekin D Cubuk, Barret Zoph, Dandelion Mane, Vijay Vasudevan, and Quoc V Le. Autoaugment: Learning augmentation policies from data. *arXiv preprint arXiv:1805.09501*, 2018. [2](#)
- [8] Wenliang Dai, Junnan Li, Dongxu Li, Anthony Meng Huat Tiong, Junqi Zhao, Weisheng Wang, Boyang Li, Pascale N Fung, and Steven Hoi. Instructblip: Towards general-purpose vision-language models with instruction tuning. *Advances in Neural Information Processing Systems*, 36, 2024. [1](#), [4](#), [5](#), [6](#), [7](#), [12](#), [17](#), [19](#), [20](#)
- [9] Ailin Deng, Zhirui Chen, and Bryan Hooi. Seeing is believing: Mitigating hallucination in large vision-language models via clip-guided decoding. *arXiv preprint arXiv:2402.15300*, 2024. [2](#)
- [10] Thomas G Dietterich. Ensemble methods in machine learning. In *International workshop on multiple classifier systems*, pages 1–15. Springer, 2000. [12](#)
- [11] Alexey Dosovitskiy, Lucas Beyer, Alexander Kolesnikov, Dirk Weissenborn, Xiaohua Zhai, Thomas Unterthiner, Mostafa Dehghani, Matthias Minderer, Georg Heigold, Sylvain Gelly, et al. An image is worth 16x16 words: Transformers for image recognition at scale. *arXiv preprint arXiv:2010.11929*, 2020. [3](#)
- [12] Alessandro Favero, Luca Zancato, Matthew Trager, Siddharth Choudhary, Pramuditha Perera, Alessandro Achille, Ashwin Swaminathan, and Stefano Soatto. Multi-modal hallucination control by visual information grounding. *arXiv preprint arXiv:2403.14003*, 2024. [2](#), [4](#), [5](#), [6](#), [7](#), [8](#), [14](#), [15](#), [16](#)
- [13] Chaoyou Fu, Peixian Chen, Yunhang Shen, Yulei Qin, Mengdan Zhang, Xu Lin, Jinrui Yang, Xiawu Zheng, Ke Li, Xing Sun, Yunsheng Wu, and Rongrong Ji. Mme: A comprehensive evaluation benchmark for multimodal large language models. *arXiv preprint arXiv:2306.13394*, 2024. [2](#), [4](#), [6](#), [7](#), [15](#), [17](#), [19](#), [21](#)
- [14] Jean-Bastien Grill, Florian Strub, Florent Althé, Corentin Tallec, Pierre Richemond, Elena Buchatskaya, Carl Doersch, Bernardo Avila Pires, Zhaohan Guo, Mohammad Gheshlaghi Azar, et al. Bootstrap your own latent—a new approach to self-supervised learning. *Advances in neural information processing systems*, 33:21271–21284, 2020. [2](#), [18](#)
- [15] Anisha Gunjal, Jihan Yin, and Erhan Bas. Detecting and preventing hallucinations in large vision language models. *arXiv preprint arXiv:2308.06394*, 2023. [2](#)
- [16] Md Zahid Hasan, Jiajing Chen, Jiyang Wang, Mohammed Shaiqur Rahman, Ameya Joshi, Senem Velipasalar, Chinmay Hegde, Anuj Sharma, and Soumik Sarkar. Vision-language models can identify distracted driver behavior from naturalistic videos. *IEEE Transactions on Intelligent Transportation Systems*, 2024. [2](#)
- [17] Ari Holtzman, Jan Buys, Li Du, Maxwell Forbes, and Yejin Choi. The curious case of neural text degeneration. *arXiv preprint arXiv:1904.09751*, 2019. [3](#)
- [18] Qidong Huang, Xiaoyi Dong, Pan Zhang, Bin Wang, Conghui He, Jiaqi Wang, Dahua Lin, Weiming Zhang, and Nenghai Yu. Opera: Alleviating hallucination in multi-modal large language models via over-trust penalty and retrospection-allocation. *arXiv preprint arXiv:2311.17911*, 2023. [1](#), [4](#), [5](#), [6](#), [7](#), [16](#)
- [19] Drew A Hudson and Christopher D Manning. Gqa: A new dataset for real-world visual reasoning and compositional question answering. In *Proceedings of the IEEE/CVF conference on computer vision and pattern recognition*, pages 6700–6709, 2019. [5](#), [6](#), [17](#), [20](#)
- [20] Chaoya Jiang, Haiyang Xu, Mengfan Dong, Jiaying Chen, Wei Ye, Ming Yan, Qinghao Ye, Ji Zhang, Fei Huang, and Shikun Zhang. Hallucination augmented contrastive learning for multimodal large language model. *arXiv preprint arXiv:2312.06968*, 2023. [2](#)
- [21] Junho Kim, Yeon Ju Kim, and Yong Man Ro. What if...?: Counterfactual inception to mitigate hallucination effects in large multimodal models. *arXiv preprint arXiv:2403.13513*, 2024. [2](#)
- [22] Masanari Kimura. Understanding test-time augmentation. In *International Conference on Neural Information Processing*, pages 558–569. Springer, 2021. [12](#)
- [23] Seongyun Lee, Sue Hyun Park, Yongrae Jo, and Minjoon Seo. Volcano: mitigating multimodal hallucination through self-feedback guided revision. *arXiv preprint arXiv:2311.07362*, 2023. [2](#)
- [24] Sicong Leng, Hang Zhang, Guanzheng Chen, Xin Li, Shijian Lu, Chunyan Miao, and Lidong Bing. Mitigating object hallucinations in large vision-language models through visual contrastive decoding. *arXiv preprint arXiv:2311.16922*, 2023. [2](#), [4](#), [5](#), [6](#), [7](#), [8](#), [14](#), [15](#), [16](#), [17](#), [18](#)
- [25] Junnan Li, Dongxu Li, Silvio Savarese, and Steven Hoi. Blip-2: Bootstrapping language-image pre-training with frozen image encoders and large language models. In *International*

- conference on machine learning, pages 19730–19742. PMLR, 2023. [3](#), [4](#), [12](#)
- [26] Wei Li, Zhen Huang, Houqiang Li, Le Lu, Yang Lu, Xinmei Tian, Xu Shen, and Jieping Ye. Visual evidence prompting mitigates hallucinations in multimodal large language models. 2023. [2](#)
- [27] Xiang Lisa Li, Ari Holtzman, Daniel Fried, Percy Liang, Jason Eisner, Tatsunori Hashimoto, Luke Zettlemoyer, and Mike Lewis. Contrastive decoding: Open-ended text generation as optimization. *arXiv preprint arXiv:2210.15097*, 2022. [15](#)
- [28] Yifan Li, Yifan Du, Kun Zhou, Jinpeng Wang, Wayne Xin Zhao, and Ji-Rong Wen. Evaluating object hallucination in large vision-language models. *arXiv preprint arXiv:2305.10355*, 2023. [1](#), [2](#), [4](#), [5](#), [6](#), [15](#), [17](#), [18](#), [19](#), [20](#), [21](#)
- [29] Yanze Li, Wenhua Zhang, Kai Chen, Yanxin Liu, Pengxiang Li, Ruiyuan Gao, Lanqing Hong, Meng Tian, Xinhai Zhao, Zhenguo Li, et al. Automated evaluation of large vision-language models on self-driving corner cases. *arXiv preprint arXiv:2404.10595*, 2024. [2](#)
- [30] Tsung-Yi Lin, Michael Maire, Serge Belongie, James Hays, Pietro Perona, Deva Ramanan, Piotr Dollár, and C Lawrence Zitnick. Microsoft coco: Common objects in context. In *Computer Vision—ECCV 2014: 13th European Conference, Zurich, Switzerland, September 6–12, 2014, Proceedings, Part V 13*, pages 740–755. Springer, 2014. [5](#), [6](#), [15](#), [16](#), [17](#), [20](#)
- [31] Fuxiao Liu, Kevin Lin, Linjie Li, Jianfeng Wang, Yaser Yacoob, and Lijuan Wang. Mitigating hallucination in large multi-modal models via robust instruction tuning. In *The Twelfth International Conference on Learning Representations*, 2023. [2](#)
- [32] Haotian Liu, Chunyuan Li, Yuheng Li, and Yong Jae Lee. Improved baselines with visual instruction tuning. *arXiv preprint arXiv:2310.03744*, 2023. [1](#), [12](#)
- [33] Haotian Liu, Chunyuan Li, Qingyang Wu, and Yong Jae Lee. Visual instruction tuning. *Advances in neural information processing systems*, 36, 2023. [1](#), [3](#), [4](#), [5](#), [6](#), [7](#), [12](#), [15](#), [16](#), [17](#), [18](#), [19](#), [20](#), [21](#), [23](#)
- [34] Junling Liu, Ziming Wang, Qichen Ye, Dading Chong, Peilin Zhou, and Yining Hua. Qilin-med-vl: Towards chinese large vision-language model for general healthcare. *arXiv preprint arXiv:2310.17956*, 2023. [2](#)
- [35] Jiaying Lu, Jinneng Rao, Kezhen Chen, Xiaoyuan Guo, Yawen Zhang, Baochen Sun, Carl Yang, and Jie Yang. Evaluation and enhancement of semantic grounding in large vision-language models. In *AAAI-ReLM Workshop*, 2024. [2](#)
- [36] OpenAI. Chatgpt interaction. Personal communication, 2023. [1](#)
- [37] Adam Paszke, Sam Gross, Francisco Massa, Adam Lerer, James Bradbury, Gregory Chanan, Trevor Killeen, Zeming Lin, Natalia Gimelshein, Luca Antiga, et al. Pytorch: An imperative style, high-performance deep learning library. *Advances in neural information processing systems*, 32, 2019. [15](#), [16](#)
- [38] Juan C Pérez, Motasem Alfarra, Guillaume Jeanneret, Laura Rueda, Ali Thabet, Bernard Ghanem, and Pablo Arbeláez. Enhancing adversarial robustness via test-time transformation ensembling. In *Proceedings of the IEEE/CVF International Conference on Computer Vision*, pages 81–91, 2021. [2](#), [12](#)
- [39] L Perez. The effectiveness of data augmentation in image classification using deep learning. *arXiv preprint arXiv:1712.04621*, 2017. [2](#)
- [40] Alec Radford, Jong Wook Kim, Chris Hallacy, Aditya Ramesh, Gabriel Goh, Sandhini Agarwal, Girish Sastry, Amanda Askell, Pamela Mishkin, Jack Clark, et al. Learning transferable visual models from natural language supervision. In *International conference on machine learning*, pages 8748–8763. PMLR, 2021. [3](#)
- [41] Anna Rohrbach, Lisa Anne Hendricks, Kaylee Burns, Trevor Darrell, and Kate Saenko. Object hallucination in image captioning. *arXiv preprint arXiv:1809.02156*, 2018. [2](#), [6](#), [7](#), [17](#), [19](#), [22](#)
- [42] Dustin Schwenk, Apoorv Khandelwal, Christopher Clark, Kenneth Marino, and Roozbeh Mottaghi. A-okvqa: A benchmark for visual question answering using world knowledge. In *European Conference on Computer Vision*, pages 146–162. Springer, 2022. [5](#), [6](#), [17](#), [20](#)
- [43] Divya Shanmugam, Davis Blalock, Guha Balakrishnan, and John Guttag. Better aggregation in test-time augmentation. In *Proceedings of the IEEE/CVF international conference on computer vision*, pages 1214–1223, 2021. [2](#), [12](#)
- [44] Connor Shorten and Taghi M Khoshgoftaar. A survey on image data augmentation for deep learning. *Journal of big data*, 6(1):1–48, 2019. [2](#)
- [45] Zhiqing Sun, Sheng Shen, Shengcao Cao, Haotian Liu, Chunyuan Li, Yikang Shen, Chuang Gan, Liang-Yan Gui, Yu-Xiong Wang, Yiming Yang, et al. Aligning large multi-modal models with factually augmented rlhf. *arXiv preprint arXiv:2309.14525*, 2023. [2](#)
- [46] Luke Taylor and Geoff Nitschke. Improving deep learning using generic data augmentation. *arXiv preprint arXiv:1708.06020*, 2017. [2](#)
- [47] Gemini Team, Rohan Anil, Sebastian Borgeaud, Yonghui Wu, Jean-Baptiste Alayrac, Jiahui Yu, Radu Soricut, Johan Schalkwyk, Andrew M Dai, Anja Hauth, et al. Gemini: a family of highly capable multimodal models. *arXiv preprint arXiv:2312.11805*, 2023. [1](#)
- [48] Hugo Touvron, Louis Martin, Kevin Stone, Peter Albert, Amjad Almahairi, Yasmine Babaei, Nikolay Bashlykov, Soumya Batra, Prajjwal Bhargava, Shruti Bhosale, et al. Llama 2: Open foundation and fine-tuned chat models. *arXiv preprint arXiv:2307.09288*, 2023. [4](#)
- [49] David Wan, Jaemin Cho, Elias Stengel-Eskin, and Mohit Bansal. Contrastive region guidance: Improving grounding in vision-language models without training. *arXiv preprint arXiv:2403.02325*, 2024. [2](#)
- [50] Bin Wang, Fan Wu, Xiao Han, Jiahui Peng, Huaping Zhong, Pan Zhang, Xiaoyi Dong, Weijia Li, Wei Li, Jiaqi Wang, et al. Vigc: Visual instruction generation and correction. *arXiv preprint arXiv:2308.12714*, 2023. [2](#)
- [51] Guotai Wang, Wenqi Li, Michael Aertsen, Jan Deprest, Sebastien Ourselin, and Tom Vercauteren. Test-time augmentation with uncertainty estimation for deep learning-based medical image segmentation. 2018. [12](#)

- [52] Guotai Wang, Wenqi Li, Michael Aertsen, Jan Deprest, Sébastien Ourselin, and Tom Vercauteren. Aleatoric uncertainty estimation with test-time augmentation for medical image segmentation with convolutional neural networks. *Neurocomputing*, 338:34–45, 2019. [12](#)
- [53] Junyang Wang, Yuhang Wang, Guohai Xu, Jing Zhang, Yukai Gu, Haitao Jia, Ming Yan, Ji Zhang, and Jitao Sang. Amber: An llm-free multi-dimensional benchmark for mllms hallucination evaluation. *arXiv preprint arXiv:2311.07397*, 2023. [1](#)
- [54] Xintong Wang, Jingheng Pan, Liang Ding, and Chris Biemann. Mitigating hallucinations in large vision-language models with instruction contrastive decoding. *arXiv preprint arXiv:2403.18715*, 2024. [2](#), [14](#)
- [55] Sam Wiseman and Alexander M Rush. Sequence-to-sequence learning as beam-search optimization. *arXiv preprint arXiv:1606.02960*, 2016. [3](#)
- [56] Peng Wu, Xuerong Zhou, Guansong Pang, Lingru Zhou, Qingsen Yan, Peng Wang, and Yanning Zhang. Vadclip: Adapting vision-language models for weakly supervised video anomaly detection. In *Proceedings of the AAAI Conference on Artificial Intelligence*, pages 6074–6082, 2024. [2](#)
- [57] Dingchen Yang, Bowen Cao, Guang Chen, and Changjun Jiang. Pensieve: Retrospect-then-compare mitigates visual hallucination. *arXiv preprint arXiv:2403.14401*, 2024. [2](#)
- [58] Qinghao Ye, Haiyang Xu, Jiabo Ye, Ming Yan, Anwen Hu, Haowei Liu, Qi Qian, Ji Zhang, and Fei Huang. mplug-owl2: Revolutionizing multi-modal large language model with modality collaboration. In *Proceedings of the IEEE/CVF Conference on Computer Vision and Pattern Recognition*, pages 13040–13051, 2024. [4](#), [5](#), [7](#), [12](#), [19](#)
- [59] Shukang Yin, Chaoyou Fu, Sirui Zhao, Tong Xu, Hao Wang, Dianbo Sui, Yunhang Shen, Ke Li, Xing Sun, and Enhong Chen. Woodpecker: Hallucination correction for multimodal large language models. *arXiv preprint arXiv:2310.16045*, 2023. [2](#)
- [60] Tianyu Yu, Yuan Yao, Haoye Zhang, Taiwen He, Yifeng Han, Ganqu Cui, Jinyi Hu, Zhiyuan Liu, Hai-Tao Zheng, Maosong Sun, et al. RLhf-v: Towards trustworthy mllms via behavior alignment from fine-grained correctional human feedback. *arXiv preprint arXiv:2312.00849*, 2023. [2](#)
- [61] Zihao Yue, Liang Zhang, and Qin Jin. Less is more: Mitigating multimodal hallucination from an eos decision perspective, 2024. [2](#)
- [62] Bohan Zhai, Shijia Yang, Chenfeng Xu, Sheng Shen, Kurt Keutzer, Chunyuan Li, and Manling Li. Halle-control: Controlling object hallucination in large multimodal models, 2024. [2](#)
- [63] Marvin Zhang, Sergey Levine, and Chelsea Finn. Memo: Test time robustness via adaptation and augmentation. *Advances in neural information processing systems*, 35:38629–38642, 2022. [2](#), [12](#)
- [64] Yi-Fan Zhang, Weichen Yu, Qingsong Wen, Xue Wang, Zhang Zhang, Liang Wang, Rong Jin, and Tieniu Tan. Debiasing large visual language models. *arXiv preprint arXiv:2403.05262*, 2024. [2](#), [14](#)
- [65] Linxi Zhao, Yihe Deng, Weitong Zhang, and Quanquan Gu. Mitigating object hallucination in large vision-language models via classifier-free guidance. *arXiv preprint arXiv:2402.08680*, 2024. [2](#)
- [66] Zhiyuan Zhao, Bin Wang, Linke Ouyang, Xiaoyi Dong, Jiaqi Wang, and Conghui He. Beyond hallucinations: Enhancing lvlms through hallucination-aware direct preference optimization. *arXiv preprint arXiv:2311.16839*, 2023. [1](#)
- [67] Hongjian Zhou, Boyang Gu, Xinyu Zou, Yiru Li, Sam S Chen, Peilin Zhou, Junling Liu, Yining Hua, Chengfeng Mao, Xian Wu, et al. A survey of large language models in medicine: Progress, application, and challenge. *arXiv preprint arXiv:2311.05112*, 2023. [2](#)
- [68] Yiyang Zhou, Chenhang Cui, Jaehong Yoon, Linjun Zhang, Zhun Deng, Chelsea Finn, Mohit Bansal, and Huaxiu Yao. Analyzing and mitigating object hallucination in large vision-language models. *arXiv preprint arXiv:2310.00754*, 2023. [2](#)
- [69] Deyao Zhu, Jun Chen, Xiaoqian Shen, Xiang Li, and Mohamed Elhoseiny. Minigpt-4: Enhancing vision-language understanding with advanced large language models. *arXiv preprint arXiv:2304.10592*, 2023. [1](#), [12](#)

Appendix

Contents

A Extended Related Work	12
B Details of RITUAL+	13
C RITUAL vs. Contrastive Decoding	14
D Detailed Experimental Settings	15
E Further Implementation Details	15
E.1. Image Transformations	15
E.2. Decoding Methods	15
F. Additional Experiments	16
F.1. Random Image Transformation vs. Single Image Transformation	16
F.2. RITUAL on Larger LVLMS	16
F.3. Compatibility of RITUAL with Contrastive Decoding Methods	16
F.4. Effect of α in RITUAL	16
F.5. Impact of One-Word Constraint	17
F.6. Effect of Transformation Intensity on Model Performance	18
F.7. Impact of the Number of Augmented Images in RITUAL	18
F.8. Detailed Performance on MME-Fullset	19
F.9. Confusion Matrices on POPE benchmark	19
F.10 Qualitative Examples	19
G Limitations	19

A. Extended Related Work

Large Vision Language Models (LVLMS). Recent approaches to integrating visual and language modalities in LVLMS commonly leverage pre-trained uni-modal models. They include an adaptive interface to bridge pre-trained visual encoders with Large Language Models (LLMs), facilitating efficient information synthesis across modalities. These interfaces generally fall into two main categories: (1) *Learnable query-based methods*, exemplified by Q-Former [25] in InstructBLIP [8] and MiniGPT-4 [69], a set of learnable query tokens is employed to capture visual signals through cross-attention. These tokens are optimized to distill the essential visual information and input it into the LLM for further processing. mPLUG-Owl2 [58] incorporates a visual abstractor that uses a predefined set of learnable queries to capture higher-level semantic features from images. (2) *Projection layer-based methods*, such as LLaVA [32, 33] and Shikra [3], use projection layers to transform visual features into the input space of LLMs. This mapping ensures seamless integration between pre-trained visual representations and the LLMs, enabling the latter to interpret the visual content effectively. Both strategies translate visual features into formats that the LLMs can understand. Despite their efficacy, LVLMS still encounter challenges with hallucination, which we aim to mitigate in this work. We specifically use three LVLMS, LLaVA, InstructBLIP, and mPLUG-Owl2, for experiments.

Test-Time Augmentation (TTA). Test-Time Augmentation (TTA) [38, 43, 51, 52, 63] enhances model robustness and generalization during inference by utilizing multiple augmented versions of an input. By applying transformations such as rotations, flips, or noise, TTA reduces uncertainty and improves accuracy through prediction averaging or ensembling across these variations. This is especially beneficial for tasks with high input variability or noise, enabling the model to handle perturbations that could otherwise degrade performance. By generating predictions for both the original and augmented inputs, TTA produces a more stable final output, mitigating the impact of noise and stabilizing predictions near decision boundaries [22]. Unlike traditional ensembling [10], which requires multiple models, TTA leverages a single model, offering the benefits of an ensemble with minimal computational cost. Our approach is similar to TTA in that we apply random transformations during inference. These augmentations broaden the model’s visual context, capturing a wider range of potential interpretations and reducing the risk of hallucinated outputs. By combining predictions from both the original and augmented inputs, we enhance robustness without additional training or complex architectures.

You are an image augmentation evaluator. Your task is to evaluate the impact of various image augmentation techniques on answering questions related to images.

Image: {Image Placeholder}

Query: {Query Placeholder}

Consider the impact of each augmentation on the understanding of an image when answering questions. Here is the list of augmentations you need to examine:

1. Horizontal flip

- Description: Reflects the image along a vertical axis, which means that the left side of the image becomes the right side, and vice versa, while the top and bottom remain unchanged.

- Pros: Can offer a different perspective without changing the semantic meaning of the content.

- Cons: May cause issues like text becoming unreadable or objects appearing in the wrong direction.

2. Vertical flip

- Description: Flips the image along a horizontal axis, creating an upside-down version while maintaining left-right orientation.

- Pros: Useful for certain artistic effects or when orientation is not critical.

- Cons: May result in unnatural-looking images, especially if the flipped orientation affects the logic of the scene, such as objects appearing in physically impossible orientations.

3. Rotation

- Description: Alters the image orientation by a certain angle.

- Pros: Enables viewing images from different angles.

- Cons: May distort image content at extreme angles, potentially leading to the loss of important features.

4. Color jitter

- Description: Introduces variations in color, including brightness, contrast, saturation, and hue.

- Pros: Useful for simulating different lighting conditions or color variations in images.

- Cons: May introduce unrealistic colors or distortions, which can be problematic for tasks where color information is critical.

5. Gaussian blur

- Description: Applies a smoothing effect, reducing noise and fine detail.

- Pros: Helps in noise reduction and focusing on more prominent features.

- Cons: May remove important details, not suitable for tasks where fine details are crucial.

6. Crop

- Description: Removes parts of the image, focusing on a specific region of interest.

- Pros: Helps in emphasizing relevant parts of the image, potentially reducing irrelevant information.

- Cons: May remove important context or details necessary for a comprehensive understanding the image.

Select the most positive augmentation that helps answer questions more accurately.

Answer always in the following form:

[Number]. [Most beneficial augmentation]

Figure 7. Prompt for RITUAL₊.

B. Details of RITUAL₊

RITUAL₊ aims to address the limitations of random image transformations. This extension is designed to minimize hallucinations and improve task-specific performance by dynamically tailoring image transformations to the query and task at hand.

Motivation. While the RITUAL leverages random image transformations to provide diverse views, these transformations often have variable impacts on model predictions. For example: (1) Gaussian Blur obscures fine details; (2) Crop reduces counting accuracy; (3) Color Jitter negatively affects color-related tasks; (4) Flips and Rotations disrupt positional understanding. To mitigate these inconsistencies and im-

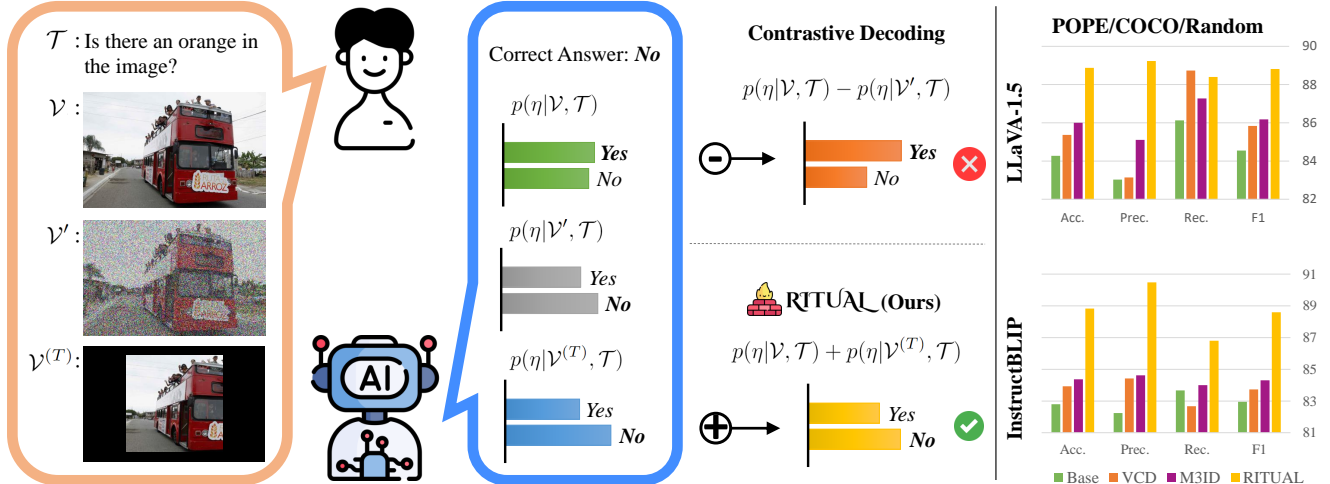


Figure 8. **Comparison of RITUAL with contrastive decoding.** Unlike contrastive decoding methods [12, 24], which contrast the conditional probability given the original image (\mathcal{V}) to that given a diffused [24] (or absent [12]) image (\mathcal{V}'), we leverage both the original image (\mathcal{V}) and a randomly transformed image ($\mathcal{V}^{(T)}$) in a complementary manner. With latency similar to contrastive decoding, RITUAL achieves state-of-the-art performance on multiple hallucination benchmarks.

prove overall reliability, RITUAL_+ employs a self-adaptive mechanism that evaluates and selects transformations based on their impact on the specific image-question pair.

Key mechanism. The process begins with the LVLM receiving an input consisting of an image and a corresponding query, such as "How many objects are in the image?" Along with this input, the model is presented with a comprehensive list of potential image transformations. Each transformation is described in detail, including its advantages and disadvantages. For instance, Gaussian Blur can improve focus by reducing noise but may obscure fine details, while Crop might emphasize specific regions of interest but risks excluding essential information.

Using this information, the LVLM evaluates each transformation in the context of the given image and query. It implicitly reasons through the pros and cons of the transformations, considering how they would affect its ability to generate an accurate response. For example, in a counting task, Gaussian Blur might reduce noise and enhances focus on prominent features, while Crop could lead to errors by excluding parts of the image critical for the task. Similarly, for positional reasoning tasks, the LVLM might reject transformations like Rotation or Flips, which could disrupt spatial orientation. Once this implicit evaluation is complete, the LVLM selects the most suitable transformation.

This query-aware transformation selection ensures that transformations are not only tailored to the input but also aligned with the task requirements, improving reliability and reducing the potential for errors. The structured reasoning process enables the model to adaptively select transformations that maximize task performance while minimizing disruptions caused by unsuitable transformations.

Prompt design. As illustrated in the prompt provided to the

LVLM (see Fig. 7), the model uses the explicit descriptions of transformations and their effects to guide its reasoning. By incorporating this self-adaptive approach, RITUAL_+ enhances the consistency and robustness of LVLM outputs, addressing the variability and unpredictability associated with random transformations.

C. RITUAL vs. Contrastive Decoding

Contrastive decoding [6, 12, 24, 54, 64] refines model outputs by contrasting two conditional probabilities: one more reliable and the other less reliable. This is typically achieved by contrasting the conditional probability of textual responses given the original visual input with that given a distorted visual input. The method aims to mitigate language biases or statistical priors, ensuring that responses are better grounded in the actual images, thereby reducing deviations from the visual truth.

While our approach also leverages two images as inputs, similar to contrastive decoding, we fundamentally differ in methodology. Instead of negatively contrasting (subtracting) the two probability distributions, we integrate them in a complementary and positive manner. Unlike contrastive decoding [12, 24, 54], which attributes hallucinations primarily to language biases or statistical priors, RITUAL proposes that hallucinatory content may stem from the visual inputs themselves. The conceptual comparison is shown in Fig. 8. In App. F.3, we also demonstrate that our method can be effectively combined with contrastive decoding techniques to achieve superior performance.

D. Detailed Experimental Settings

POPE⁵. We utilize the official benchmark from [28], which includes 3,000 question-answer pairs for each of the random, popular, and adversarial settings. We use the query template ‘Is there a [object] in the image?’. Here, [object] is selected randomly, from the most frequent objects in the dataset, or from objects that frequently co-occur with [object], corresponding to the random, popular, and adversarial settings respectively. We evaluate the performance based on whether the model-generated output contained the ground truth (‘Yes’ or ‘No’) using accuracy, precision, recall, and average F1-score.

MME⁶. The MME [13] dataset consists of 10 perception categories (existence, count, position, color, posters, celebrity, scene, landmark, artwork, OCR) and 4 recognition ones (commonsense reasoning, numerical calculation, text translation, code reasoning). Each query is used with an image-related question followed by "Please answer yes or no." We report the sum of accuracy at the query level and image level following the official implementation.

CHAIR⁷. We select 500 random images from the COCO [30] validation set and generate the output using the query "Please describe this image in detail.". Due to the computational complexity, we restrict the *max new tokens* to 64. Following the M3ID [12], we report two assessment metrics, C_s and C_i , which calculate the hallucination ratio per sentence and instance as follows:

$$C_s = \frac{|\{\text{sentences with hallucinated objects}\}|}{|\{\text{all sentences}\}|}, \quad (5)$$

$$C_i = \frac{|\{\text{hallucinated objects}\}|}{|\{\text{all objects mentioned}\}|}. \quad (6)$$

LLaVA-Bench⁸. The LLaVA-Bench [33] dataset consists of 24 images along with 60 image-related questions. This dataset is demanding as it has been collected from a variety of domains including diverse scenes, memes, paintings, sketches, and more. We conduct qualitative case studies on this dataset to exhibit the efficacy of RITUAL in challenging tasks and its adaptability to new domains.

E. Further Implementation Details

E.1. Image Transformations

We set predefined six commonly used image transformations and randomly applied one of them for each image. We provide a concise description and implementation details below. We employ the Pytorch/Torchvision [37] implementation for transformation.

⁵<https://github.com/RUCAIBox/POPE>

⁶<https://github.com/BradyFU/Awesome-Multimodal-Large-Language-Models/tree/Evaluation>

⁷<https://github.com/LisaAnne/Hallucination>

⁸<https://huggingface.co/datasets/liuhaotian/llava-bench-in-the-wild>

Horizontal flip flips the image in the horizontal direction.

Vertical flip flips the image in the vertical direction.

Rotation rotates the image by a selected angle. The rotation angle is uniformly sampled from the *degrees*=(−180, +180).

Color jitter adjusts the brightness, contrast, saturation, and hue of the image. We set *brightness*=1, *contrast*=1, *saturation*=1, *hue*=0.5.

Gaussian blur applies Gaussian blurring to the image with a chosen standard deviation *sigma*. We set *kernel_size*=13 and *sigma*=(1.5, 2.0).

Random Resized Crop randomly crops a region of the image and resizes it to a specified size. We set *size*=336 as the same as the original data resize scale.

E.2. Decoding Methods

For a fair comparison, we adopt an adaptive plausible constraint based on the confidence level associated with the output distribution derived from the original visual inputs, following [24, 27]. The plausible constraint is defined as:

$$\mathcal{O}(\eta_{<t}) = \left\{ \eta_t \in \mathcal{O} : p_\theta(\eta_t | \mathcal{V}, \mathcal{T}, \eta_{<t}) \geq \beta \right. \\ \left. \times \max_w p_\theta(w | v, x, y_{<t}) \right\}. \quad (7)$$

where \mathcal{O} represents the output vocabulary of LVLm, and β is a hyperparameter for the plausible constraint that adjusts truncation of the next token distribution. The logits of tokens not in \mathcal{O} are set $-\infty$, meaning that a larger β retains only tokens with higher probabilities. For all experiments, we set $\beta=0.1$. We configured the hyperparameter with a value of $\alpha = 3$ in Eq. 4 by default. Note that we reproduced VCD [24] and M3ID [12] under our experimental settings. Specifically, we used the contrastive distribution of VCD as shown below:

$$\eta_t^{\text{VCD}} \sim \gamma p_\theta(\eta_t | \mathcal{V}, \mathcal{T}, \eta_{<t}) - \delta p_\theta(\eta_t | \mathcal{V}', \mathcal{T}, \eta_{<t}). \quad (8)$$

where \mathcal{V}' represents a corrupted version of the original image \mathcal{V} . We set the balancing parameters $\gamma = 2$, $\delta = 1$, and the total noise steps to 500 for generating \mathcal{V}' .

For M3ID, a key concept to prevent conditioning dilution is reproduced by introducing an unconditioned model as follows:

$$\eta_t^{\text{M3ID}} \sim p_\theta(\eta_t | \mathcal{V}, \mathcal{T}, \eta_{<t}) + \frac{1 - e^{-\lambda t}}{e^{-\lambda t}} \left(p_\theta(\eta_t | \mathcal{V}, \mathcal{T}, \eta_{<t}) - p_\theta(\eta_t | \mathcal{T}, \eta_{<t}) \right). \quad (9)$$

Here, λ is a parameter balancing the conditioned and unconditioned models, set to 0.1 in our experiments. For RITUAL combined with contrastive decoding, we used a combined distribution:

$$\zeta \eta_t^{(T)} + \eta_t^D, \quad \text{where} \{ \text{VCD, M3ID} \} \in D, \quad (10)$$

and $\eta_t^{(T)} = p_\theta(\eta_t | \mathcal{V}^{(T)}, \mathcal{T}, \eta_{<t})$. In this setup, we set $\gamma = 1$, $\delta = 0.1$, and $\zeta = 3$ for `RITUAL` with VCD, and $\lambda = 0.1$ and $\zeta = 3.5$ for `RITUAL` with M3ID. In the case of DoLa [6], we select the first bucket of candidate layers. For OPERA [18], we set the scale factor to 50, the threshold to 15, the number of attention candidates to 5, penalty weights to 1, and the number of beams to 5. The code is implemented in Python 3.10 with PyTorch 2.0.1 [37], and all experiments are conducted with a single NVIDIA RTX 3090 GPU.

F. Additional Experiments

F.1. Random Image Transformation vs. Single Image Transformation

Table 8. Performance of singular and random image transformations on POPE COCO benchmark.

Setup	Transformation	LLaVA 1.5 [33]			
		Acc. \uparrow	Prec. \uparrow	Rec. \uparrow	F1 \uparrow
Random	Horizontal Flip	89.50	89.95	88.93	89.44
	Vertical Flip	88.60	88.76	88.40	88.58
	Rotate	88.90	89.56	88.07	88.81
	Color Jitter	88.83	89.98	87.40	88.67
	Gaussian Blur	88.77	89.48	87.87	88.66
	Crop	88.47	89.36	87.33	88.33
	Random Selection	88.87	89.23	88.40	88.58
Popular	Horizontal Flip	85.60	83.21	89.20	86.10
	Vertical Flip	85.23	83.05	88.53	85.71
	Rotate	86.20	84.67	88.40	86.50
	Color Jitter	86.20	84.90	88.07	86.45
	Gaussian Blur	84.93	83.29	87.40	85.30
	Crop	85.70	84.62	87.27	85.92
	Random Selection	85.83	84.17	88.27	86.17
Adversarial	Horizontal Flip	79.50	74.65	89.33	81.34
	Vertical Flip	79.10	74.65	88.13	80.83
	Rotate	79.73	75.06	89.07	81.46
	Color Jitter	78.70	74.47	87.33	80.39
	Gaussian Blur	78.73	74.19	88.13	80.56
	Crop	79.37	75.48	87.00	80.83
	Random Selection	78.80	74.43	87.73	80.54

To generate transformed images $\mathcal{V}^{(T)}$, we randomly apply one of six image transformations: horizontal flip, vertical flip, rotate, color jitter, Gaussian blur, or crop. We compare this random selection with a method that only adopts specific transformations rather than making a random choice. As shown in Table 8, the effectiveness of each transformation varies significantly depending on the POPE evaluation setup. For instance, in the popular setup, applying color jitter exclusively achieves the best results across most metrics (Acc: 86.20, Prec: 84.90, Rec: 88.07, F1: 86.45). In contrast, the same transformation delivers the poorest results in the adversarial setup, where it leads to lower F1 scores (80.39). Similarly, transformations like horizontal flip, rotation, and Gaussian blur also demonstrate inconsistent impacts, being effective in one context while detrimental in another. These results underscore the variability and task-specific nature of

transformations. The same transformation can yield either beneficial or harmful outcomes depending on the specific image-query pair and evaluation scenario. To address this inherent randomness and its potential drawbacks, we propose `RITUAL+`, a self-adaptive framework that dynamically selects the most suitable transformation based on task requirements and feedback.

F.2. `RITUAL` on Larger LLMs

Table 9. Results of 13B models on POPE COCO benchmark.

Setup	Method	LLaVA-1.5 (13B)				InstructBLIP (13B)			
		Acc.	Prec.	Rec.	F1	Acc.	Prec.	Rec.	F1
Random	base	82.70	78.73	89.60	83.82	80.10	75.21	89.80	81.86
	VCD	82.97	79.00	89.80	84.06	82.83	78.65	90.13	84.00
	M3ID	84.53	80.51	91.13	85.49	81.57	76.56	91.00	83.16
	<code>RITUAL</code>	87.03	83.69	92.00	87.65	84.87	78.49	96.07	86.39
	base	80.93	76.95	88.33	82.25	75.80	70.14	89.87	78.78
Popular	VCD	80.23	75.58	89.33	81.88	77.43	71.56	91.07	80.14
	M3ID	81.57	76.92	90.20	83.03	76.43	70.22	91.80	79.57
	<code>RITUAL</code>	84.57	80.20	91.80	85.61	78.43	71.23	95.40	81.56
	base	75.90	70.76	88.27	78.55	71.47	65.48	90.80	76.09
Adversarial	VCD	75.63	69.83	90.27	78.74	73.33	67.45	90.20	77.18
	M3ID	78.77	73.09	91.07	81.09	71.40	65.29	91.40	76.17
	<code>RITUAL</code>	77.93	71.75	92.13	80.68	72.37	65.37	95.13	77.49

We report the results of the LLaVA-v1.5-13B and InstructBLIP-13B models on the POPE benchmark using the COCO dataset in Table 9. `RITUAL` achieves the best overall performance across most metrics and settings, particularly excelling in the random and popular dataset types. Although its performance slightly falls short of VCD and M3ID under the adversarial setting, its superiority in other types suggests its robustness and effectiveness.

F.3. Compatibility of `RITUAL` with Contrastive Decoding Methods

As shown in Tables 10 to 12, `RITUAL` yields further performance improvement when incorporated with contrastive decoding methods, such as VCD [24] and M3ID [12], across various benchmarks. This compatibility demonstrates a synergy between the two approaches. While contrastive decoding primarily mitigates language biases by contrasting conditional probabilities, `RITUAL` enriches visual understanding by leveraging transformations to capture diverse visual contexts. Together, these methods effectively address the problem of object hallucinations and improve model grounding.

F.4. Effect of α in `RITUAL`

In Table 13, we conduct an ablation study on the hyperparameter α in Eq. 4, which adjusts the ratio between the output logits of the model conditioned on the original image \mathcal{V} and the transformed image $\mathcal{V}^{(T)}$. We vary α from 0 (standard decoding) to 3.5 on the POPE COCO random setting. Our method consistently outperforms the baseline across a broad spectrum of α values, with accuracy improvement ranging from +3.60 to +4.74. This demonstrates that our approach is robust and effective regardless of the specific hyperparameter value chosen. Based on these results, we set $\alpha = 3$ as the default value.

Table 10. Compatibility with contrastive decoding on POPE benchmark [28].

Setup	Method	LLaVA 1.5 [33]				InstructBLIP [8]				
		Acc. \uparrow	Prec. \uparrow	Rec. \uparrow	F1 \uparrow	Acc. \uparrow	Prec. \uparrow	Rec. \uparrow	F1 \uparrow	
MS-COCO [30]	Random	RITUAL	88.87	89.23	88.40	88.81	88.83	90.48	86.80	88.60
		+VCD	89.07	89.49	88.53	89.01	89.30	90.85	87.40	89.09
		+M3ID	89.00	89.85	87.93	88.88	88.93	91.13	86.27	88.63
	Popular	RITUAL	85.83	84.17	88.27	86.17	81.97	78.90	87.27	82.87
		+VCD	85.77	83.89	88.53	86.15	82.83	80.16	87.27	83.56
		+M3ID	85.37	83.60	88.00	85.74	81.90	78.98	86.93	82.77
	Adversarial	RITUAL	78.80	74.43	87.73	80.54	78.73	74.57	87.20	80.39
		+VCD	79.60	75.26	88.20	81.22	79.07	74.89	87.47	80.69
		+M3ID	79.20	74.83	88.00	80.88	78.93	75.06	86.67	80.45
A-OKVQA [42]	Random	RITUAL	85.17	79.79	94.20	86.40	87.13	83.92	91.87	87.71
		+VCD	85.10	79.93	93.73	86.28	86.77	83.57	91.53	87.37
		+M3ID	85.93	80.62	94.60	87.06	87.17	84.35	91.27	87.67
	Popular	RITUAL	78.83	71.99	94.40	81.68	78.73	72.83	91.67	81.17
		+VCD	79.17	72.40	94.27	81.90	78.83	72.75	92.20	81.33
		+M3ID	79.63	72.83	94.53	82.27	79.20	73.42	91.53	81.48
	Adversarial	RITUAL	68.57	62.26	94.27	74.99	70.27	64.15	91.87	75.55
		+VCD	68.80	62.48	94.13	75.11	71.00	64.72	92.33	76.10
		+M3ID	68.77	62.42	94.33	75.13	69.30	63.43	91.13	74.80
GQA [19]	Random	RITUAL	86.10	80.30	95.67	87.31	84.87	82.52	88.47	85.39
		+VCD	86.03	80.21	95.67	87.26	84.97	82.40	88.93	85.54
		+M3ID	86.30	80.64	95.53	87.46	85.00	82.94	88.13	85.46
	Popular	RITUAL	74.80	67.50	95.67	79.15	74.50	69.17	88.40	77.61
		+VCD	75.07	67.82	95.40	79.28	75.33	69.98	88.73	78.25
		+M3ID	74.40	67.15	95.53	78.87	75.57	70.24	88.73	78.41
	Adversarial	RITUAL	68.23	61.75	95.80	75.10	70.17	64.76	88.47	74.78
		+VCD	69.00	62.39	95.67	75.53	70.23	64.81	88.53	74.84
		+M3ID	68.80	62.29	95.27	75.33	71.00	65.32	89.53	75.53

Table 11. Compatibility with contrastive decoding on MME-Hallucination benchmark [13].

Model	Method	Object-level		Attribute-level		Total Score
		Existence \uparrow	Count \uparrow	Position \uparrow	Color \uparrow	
LLaVA 1.5	RITUAL	187.50(± 2.89)	139.58(± 7.62)	125.00(± 10.27)	164.17(± 6.87)	616.25(± 20.38)
	+VCD	185.00(± 4.08)	140.84(± 4.41)	125.00(± 7.07)	165.83(± 6.46)	616.67(± 11.14)
	+M3ID	187.50(± 2.89)	141.25(± 9.85)	125.00(± 10.27)	164.17(± 6.87)	617.92(± 22.12)
InstructBLIP	RITUAL	182.50(± 6.45)	74.58(± 5.99)	67.08(± 10.31)	139.17(± 0.96)	463.33(± 12.40)
	+VCD	185.00(± 4.08)	75.00(± 7.07)	62.50(± 6.46)	141.67(± 6.53)	464.17(± 9.07)
	+M3ID	182.50(± 6.45)	74.58(± 2.84)	63.33(± 11.55)	140.42(± 2.10)	460.83(± 11.1)

F.5. Impact of One-Word Constraint

One of our primary baseline methods, VCD [24], introduces an additional instruction at the end of each question: "Please answer this question with one word". As shown in Table 14, this constraint biases the model towards shorter, more definitive answers, with a notable inclination towards "No" (resulting in a 60% No ratio). In contrast, our evaluation setup removes this "one-word" constraint, allowing the model to

generate more detailed responses that include explanations. This approach results in a more balanced distribution of "Yes" and "No" answers (approximately 50% each). Rather than limiting the output to a single word for simplicity in evaluation, our method assesses whether the response contains a "Yes" or "No" alongside a supporting explanation. Despite this adjustment, RITUAL achieves the best performance on the primary metric, F1, highlighting its effectiveness. Note that since there is no official implementation of M3ID, we

Table 12. Compatibility with contrastive decoding on CHAIR benchmark [41].

	Method	CHAIR _S \downarrow	CHAIR _L \downarrow
LLaVA 1.5	RITUAL	20.6	6.9
	+VCD	20.0	6.8
	+M3ID	18.0	5.7
InstructBLIP	RITUAL	26.0	8.8
	+VCD	25.0	8.6
	+M3ID	23.4	7.9

Table 13. **Impact of α on POPE [28] COCO random benchmark.** Based on the results, we set $\alpha = 3$ as the default.

α	LLaVA 1.5 [33]			
	Acc. \uparrow	Prec. \uparrow	Rec. \uparrow	F1 \uparrow
0 (<i>base</i>)	84.13	82.86	86.07	84.43
0.5	87.73	87.04	88.67	87.85
1	88.00	87.70	88.40	88.05
1.5	88.53	88.74	88.27	88.50
2	88.50	89.05	87.80	88.42
2.5	88.27	88.68	87.73	88.20
3	88.87	89.23	88.40	88.81
3.5	88.67	89.40	87.73	88.56

Table 14. **Impact of the one-word constraint on POPE COCO random benchmark.** In constrained setup, we use additional query "Please answer this question in one word."

One word Constraint	Method	LLaVA 1.5 [33]				
		Yes Ratio	Acc.	Prec.	Rec.	F1
✓	<i>base</i>	39.90	83.29	92.13	72.80	81.33
	VCD	40.97	87.73	91.42	83.28	87.16
✗	<i>base</i>	51.87	84.13	82.86	86.07	84.43
	VCD	53.37	85.37	83.14	88.73	85.84
	M3ID	50.97	86.00	85.11	87.27	86.18
	DoLa	51.23	85.97	85.10	87.20	86.14
	RITUAL	49.53	88.87	89.23	88.40	88.81

reimplemented the method and reported its results based on our settings.

F.6. Effect of Transformation Intensity on Model Performance

Table 15. **Performance of RITUAL with Gaussian noise at different noise steps and VCD with Gaussian blur at different sigma values on POPE COCO random benchmark.**

(a) RITUAL w/ Gaussian noise.					
Noise Step	LLaVA 1.5 [33]				
	Acc.	Prec.	Rec.	F1	
50	89.37	91.04	87.33	89.15	
999	81.47	75.85	92.33	83.28	
(b) VCD w/ Gaussian blur.					
Sigma	LLaVA 1.5 [33]				
	Acc.	Prec.	Rec.	F1	
0.5	83.77	83.61	84.00	83.80	
100	85.13	86.45	83.33	84.86	

In our work, we use standard image transformations (*e.g.*, crop, flip, rotate, color jitter, and Gaussian blur) to enhance model robustness by generating diverse views [4, 14]. The key principle is that applying these transformations at an *appropriate intensity* creates diverse perspectives while pre-

serving the underlying semantics of the image.

Contrastive decoding methods, such as VCD [24], leverage Gaussian noise to distort images and contrast probability distributions between the original and distorted versions. VCD applies high-intensity noise (*e.g.*, diffusion noise steps of 500 or 999, where 1000 steps typically reduce an image to near-complete Gaussian noise). In contrast, RITUAL employs low to moderate-intensity transformations, combining the probability distributions of the original and transformed images in a complementary manner.

RITUAL w/ Gaussian noise. To explore how Gaussian noise, as used in VCD, performs as an image transformation, we applied it within the RITUAL framework on the POPE-COCO-random setup (Table 15a). At low noise intensities (*e.g.*, noise step = 50), Gaussian noise effectively generates diverse perspectives while preserving the image’s semantic integrity, leading to enhanced performance. However, at high noise intensities (*e.g.*, noise step = 999), the transformation overly distorts the image, degrading performance by obscuring its content. These results highlight the dependency of Gaussian noise’s efficacy on its intensity: low levels promote beneficial diversity, whereas excessive noise impairs understanding.

VCD w/ Gaussian blur. We also evaluate VCD with Gaussian blur at different sigma values (Table 15b). Low sigma value ($\sigma = 0.5$) introduces minimal blur while preserving image semantics, whereas high sigma value ($\sigma = 100$) causes significant distortion. VCD contrasts the probability distributions of the original and distorted images to reduce language prior influence and enhance visual grounding. Stronger blur shifts the focus to visual content, mitigating object hallucination and improving performance in visually grounded tasks.

F.7. Impact of the Number of Augmented Images in RITUAL

Table 16. **Impact of the number of augmented images in RITUAL on POPE COCO benchmark.**

Setup	# of Aug. Images	LLaVA-1.5 [33]			
		Acc.	Prec.	Rec.	F1
Random	1	88.87	89.23	88.40	88.81
	2	89.07	89.38	88.67	89.02
	3	89.17	89.25	89.07	89.16
Popular	1	85.83	84.17	88.27	86.17
	2	85.37	83.85	87.60	85.69
	3	86.20	84.11	89.27	86.61
Adversarial	1	78.80	74.43	87.73	80.54
	2	79.10	74.56	88.33	80.87
	3	79.07	74.63	88.07	80.80

As shown in Table 16, we found that performances slightly improve with the addition of more augmented images. This improvement is likely due to the increased variety

Table 17. Results on MME-Fullset [13].

Task	Category	LLaVA 1.5 [33]						InstructBLIP [8]						mPLUG-Owl2 [58]						
		base	VCD	M3ID	DoLa	RITUAL	RITUAL ₊	base	VCD	M3ID	DoLa	RITUAL	RITUAL ₊	base	VCD	M3ID	DoLa	RITUAL	RITUAL ₊	
Perception	Existence	173.75 (±4.79)	178.75 (±2.5)	177.50 (±6.45)	174.58 (±5.34)	187.50 (±2.89)	188.89 (±6.74)	160.42 (±5.16)	158.75 (±7.25)	158.33 (±5.44)	162.08 (±5.34)	182.50 (±6.45)	187.20 (±5.09)	174.58 (±4.17)	170.00 (±0.00)	176.25 (±4.79)	175.00 (±5.77)	185.00 (±4.08)	189.44 (±5.09)	
	Count	121.67 (±12.47)	126.25 (±10.4)	124.17 (±10.93)	122.09 (±11.73)	139.58 (±7.62)	145.55 (±2.55)	79.17 (±8.22)	90.75 (±3.11)	94.58 (±9.85)	82.50 (±6.16)	74.58 (±5.99)	88.89 (±13.47)	155.42 (±10.03)	138.75 (±6.44)	157.92 (±9.75)	151.67 (±5.61)	159.58 (±13.57)	159.45 (±5.36)	
	Position	117.92 (±7.51)	120.00 (±11.01)	120.00 (±5.67)	122.09 (±4.19)	125.00 (±4.19)	164.17 (±6.87)	110.00 (±10.58)	79.58 (±17.34)	70.00 (±18.78)	72.50 (±17.03)	78.75 (±14.72)	67.08 (±0.96)	72.22 (±10.93)	81.67 (±13.29)	81.25 (±5.51)	81.67 (±12.51)	82.09 (±5.51)	77.50 (±4.59)	83.33 (±8.55)
	Color	149.17 (±3.69)	150.83 (±4.08)	152.92 (±7.07)	149.17 (±2.10)	164.17 (±10.27)	173.89 (±10.58)	130.42 (±8.54)	132.5 (±15.81)	128.33 (±17.03)	135.42 (±14.72)	139.17 (±10.49)	148.33 (±10.93)	141.25 (±13.29)	138.75 (±5.51)	142.50 (±12.51)	139.58 (±5.51)	160.42 (±14.72)	162.22 (±14.17)	
	Posters	124.24 (±3.36)	129.34 (±4.11)	120.49 (±3.23)	127.98 (±5.51)	135.46 (±0.94)	133.79 (±2.27)	101.96 (±1.5)	114.29 (±7.07)	110.54 (±0.62)	105.10 (±3.41)	139.46 (±4.85)	142.97 (±9.91)	154.08 (±3.24)	150.79 (±5.53)	154.76 (±4.01)	150.45 (±3.94)	158.39 (±2.60)	141.61 (±11.33)	
	Celebrity	115.44 (±3.98)	124.78 (±6.23)	113.9 (±1.8)	115.00 (±8.20)	120.07 (±1.88)	122.16 (±2.94)	105.22 (±2.23)	128.31 (±5.14)	119.05 (±5.01)	150.74 (±2.15)	134.63 (±4.19)	136.37 (±9.07)	152.16 (±4.19)	158.33 (±3.56)	152.16 (±3.51)	144.70 (±1.06)	147.06 (±4.12)	145.49 (±1.67)	
	Scene	147.44 (±6.26)	152.69 (±2.46)	155.94 (±2.83)	150.94 (±1.21)	159.75 (±2.79)	154.75 (±3.25)	130.19 (±3.9)	140.56 (±3.78)	145.31 (±4.98)	147.75 (±2.62)	158.63 (±7.94)	165.75 (±2.14)	153.75 (±2.74)	150.33 (±2.08)	154.33 (±1.38)	154.08 (±1.38)	159.67 (±8.63)	168.92 (±8.63)	
	Landmark	133.31 (±4.73)	136.00 (±7.35)	133.81 (±5.84)	132.31 (±6.20)	157.81 (±2.19)	161.25 (±4.44)	118.13 (±3.37)	131.06 (±7.71)	127.06 (±3.08)	126.31 (±1.89)	150.69 (±10.90)	152.25 (±5.38)	145.92 (±4.93)	136.08 (±4.42)	146.75 (±2.27)	140.83 (±3.26)	156.17 (±3.26)	152.17 (±16.96)	
	Artwork	107.31 (±2.61)	110.50 (±0.79)	111.69 (±0.92)	107.25 (±7.95)	117.31 (±2.23)	126.92 (±6.21)	91.44 (±4.24)	102.75 (±3.91)	98.44 (±4.31)	117.44 (±6.95)	103.94 (±12.00)	113.42 (±0.80)	128.92 (±1.15)	131.25 (±0.29)	130.42 (±0.43)	129.75 (±2.32)	133.08 (±2.32)	128.92 (±4.73)	
	OCR	107.50 (±13.99)	98.13 (±7.18)	112.50 (±10.21)	97.50 (±10.80)	121.25 (±6.29)	119.17 (±10.41)	90.63 (±6.88)	81.25 (±6.61)	78.75 (±17.85)	73.13 (±8.00)	93.75 (±8.29)	111.67 (±3.82)	102.50 (±7.50)	110.00 (±12.99)	102.50 (±7.50)	100.00 (±4.33)	105.00 (±4.33)	105.83 (±9.46)	
Recognition	Commonsense Reasoning	99.82 (±9.39)	108.04 (±2.36)	107.32 (±10.13)	107.32 (±8.98)	115.54 (±4.92)	119.52 (±6.87)	92.68 (±8.64)	92.86 (±6.20)	96.43 (±6.31)	96.43 (±8.17)	109.11 (±8.17)	100.83 (±28.10)	118.33 (±6.63)	115.24 (±1.80)	117.62 (±5.45)	118.10 (±5.46)	121.19 (±4.76)	128.79 (±5.49)	
	Numerical Calculation	60.00 (±12.42)	63.75 (±8.54)	68.75 (±7.22)	64.38 (±12.64)	52.50 (±8.9)	66.67 (±13.77)	56.88 (±15.6)	64.38 (±6.25)	60.63 (±19.51)	56.88 (±11.97)	63.75 (±9.24)	83.33 (±15.07)	43.33 (±16.07)	46.67 (±10.41)	43.33 (±16.07)	48.33 (±20.36)	45.83 (±8.78)	75.00 (±10.00)	
	Text Translation	81.88 (±13.13)	77.50 (±8.90)	87.50 (±10.61)	81.25 (±8.78)	93.75 (±10.51)	87.50 (±0.00)	56.88 (±17.49)	66.25 (±6.61)	72.50 (±12.75)	74.38 (±10.48)	89.38 (±12.48)	76.67 (±8.78)	90.00 (±7.50)	76.67 (±15.07)	90.00 (±7.50)	89.17 (±15.07)	84.17 (±7.64)	85.00 (±16.39)	
	Code Reasoning	64.38 (±25.93)	63.75 (±25.86)	64.38 (±25.93)	64.38 (±29.04)	65.00 (±10.21)	73.33 (±6.29)	63.75 (±11.27)	72.50 (±20.31)	78.13 (±15.33)	70.00 (±7.91)	66.19 (±8.61)	70.00 (±4.08)	60.00 (±10.90)	62.50 (±17.50)	60.00 (±10.90)	57.50 (±7.50)	71.67 (±14.43)	67.50 (±16.39)	

of views available for the same scene, enhancing the model’s generalization ability. However, it is important to note that this also leads to increased computational overhead due to the necessity of additional forward passes. Using multiple augmented images can indeed contribute to performance improvement, but it comes with the inherent trade-off of increased latency due to the additional computational cost.

F.8. Detailed Performance on MME-Fullset

Table 17 presents the results on the MME-Fullset benchmark [13]. We compare the decoding methods applied to several LLMs, including LLaVA-1.5 [33], InstructBLIP [8], and mPLUG-Owl2 [58]. Across all tested models, RITUAL and RITUAL₊ demonstrate consistent and significant improvements on most task categories, showcasing its effectiveness in enhancing LLMs’ ability to accurately interpret and analyze general visual contents. RITUAL delivers significant performance gains by enhancing the models’ ability to interpret and analyze visual content accurately. RITUAL₊ further boosts results through adaptive transformation selection, showcasing its ability to tailor transformations for specific tasks and use cases. In perception tasks, RITUAL and RITUAL₊ outperform baseline methods in categories such as Existence, Count, and Landmark. In recognition tasks, they excel in Commonsense Reasoning and Text Translation, achieving top scores across multiple LLMs.

F.9. Confusion Matrices on POPE benchmark

To analyze the performance of the model in detail, we report the confusion matrices in Table 18 for the POPE benchmark. Notably, RITUAL significantly improves True Negatives (TN) while maintaining a similar level of True Positives (TP) compared to existing contrastive decoding methods. It implies that our method achieves the highest accuracy by

significantly improving the identification of non-relevant instances compared to the baseline and previous methods.

F.10. Qualitative Examples

We provide additional qualitative examples on POPE [28], MME [13], CHAIR [41], and LLaVA-Bench [33] in Figs. 9 to 13.

Fig. 9 presents two samples from the LLaVA-Bench [33] with LLaVA-1.5 [33], highlighting the differences between sentences generated by standard decoding (Base) and those produced by RITUAL. The results demonstrate that standard decoding often results in hallucinations, which can be effectively rectified by implementing RITUAL. For instance, in the left-hand image, the baseline model incorrectly identifies a ‘street vendor’ and ‘initiative signs’, neither of which are present in the image. Additionally, it misinterprets ‘ironing’ as ‘doing laundry’. In the right-hand image, the baseline model hallucinates objects not present in the image, such as a ‘hat’, ‘paint mustache’, and ‘two more dogs’. In contrast, our approach helps counteract these hallucinations, generating sentences that reflect a more accurate comprehension of the image.

G. Limitations

RITUAL is a simple yet effective technique that improves model robustness against hallucinations. However, it comes with the following limitations:

- **Computational overhead:** RITUAL necessitates running the model twice for each test image, resulting in higher inference time and computational demands. This can pose challenges in real-time or resource-constrained scenarios.
- **Diminishing returns:** Although RITUAL offers noticeable performance gains, its benefits taper off with exces-

Table 18. Confusion matrices on POPE [28] benchmark.

Setup	Method	LLaVA 1.5 [33]					InstructBLIP [8]					
		TP \uparrow	FP \downarrow	TN \uparrow	FN \downarrow	Acc. \uparrow	TP \uparrow	FP \downarrow	TN \uparrow	FN \downarrow	Acc. \uparrow	
MS-COCO [30]	Random	<i>base</i>	1291	267	1233	209	84.13	1255	271	1229	245	82.80
		VCD	1331	270	1230	169	85.37	1240	222	1278	260	83.93
		M3ID	1309	229	1271	191	86.00	1260	229	1271	240	84.37
		RITUAL	1326	160	1340	174	88.87	1302	137	1363	198	88.83
	Popular	<i>base</i>	1283	357	1143	217	80.87	1238	464	1036	262	75.80
		VCD	1306	373	1127	194	81.10	1234	402	1098	266	77.73
		M3ID	1324	339	1161	176	82.83	1259	440	1060	241	77.30
		Ours	1324	249	1251	176	85.83	1309	350	1150	191	81.97
	Adversarial	<i>base</i>	1298	511	989	202	76.23	1263	501	999	237	75.40
		VCD	1308	540	960	192	75.60	1253	449	1051	247	76.80
		M3ID	1310	479	1021	190	77.70	1259	478	1022	241	76.03
		RITUAL	1316	452	1048	184	78.80	1308	446	1054	192	78.73
A-OKVQA [42]	Random	<i>base</i>	1373	421	1079	127	81.73	1300	366	1134	200	81.13
		VCD	1405	450	1050	95	81.83	1297	337	1163	203	82.00
		M3ID	1407	400	1100	93	83.57	1357	387	1113	143	82.33
		RITUAL	1413	358	1142	87	85.17	1378	264	1236	122	87.13
	Popular	<i>base</i>	1375	575	925	125	76.67	1303	533	967	197	75.67
		VCD	1393	652	848	107	74.70	1314	519	981	186	76.50
		M3ID	1416	551	949	84	78.83	1375	513	987	125	78.73
		RITUAL	1416	551	949	84	78.83	1375	513	987	125	78.73
	Adversarial	<i>base</i>	1369	847	653	131	67.40	1302	762	738	198	68.00
		VCD	1400	877	623	100	67.43	1327	707	793	173	70.67
		M3ID	1404	861	639	96	68.10	1326	739	761	174	69.57
		RITUAL	1414	857	643	86	68.57	1378	770	730	122	70.27
GQA [19]	Random	<i>base</i>	1390	453	1047	110	81.23	1289	391	1109	211	79.93
		VCD	1426	481	1019	74	81.50	1300	345	1155	200	81.83
		M3ID	1417	432	1068	83	82.83	1315	398	1102	185	80.57
		RITUAL	1435	352	1148	65	86.10	1327	281	1219	173	84.87
	Popular	<i>base</i>	1402	727	773	98	72.50	1281	599	901	219	72.73
		VCD	1422	775	725	78	71.57	1298	588	912	202	73.67
		M3ID	1410	725	775	90	72.83	1316	579	921	184	74.57
		RITUAL	1435	691	809	65	74.80	1326	591	909	174	74.50
	Adversarial	<i>base</i>	1397	868	632	103	67.63	1285	698	802	215	69.57
		VCD	1413	889	611	87	67.47	1279	696	804	221	69.43
		M3ID	1417	873	627	83	68.13	1292	725	775	208	68.90
		RITUAL	1437	890	610	63	68.23	1327	722	778	173	70.17

sive or redundant transformations, which may introduce unnecessary complexity without significant improvements.


Query: What is unusual about this image?



Base: The unusual aspect of this image is a person, most likely a **street vendor**, **doing laundry** on the back of a taxi cab while it is in motion on a city street. A blue sheet or **initiative sign** is also hanging off the **truck owned by this street vendor**. The activity of **laundry** being done in a public vehicle while on the move is not a common sight in urban environments and likely draws attention, as it is an unconventional and perhaps unorthodox approach to carrying out such tasks.

RITUAL: The unusual aspect of this image is that a man is ironing clothes while standing on the back of a moving taxi. This is not a typical scenario, as ironing clothes is usually done indoors, in a more controlled environment, and not while traveling in a vehicle. The man's choice to iron clothes in a moving taxi adds an element of unconventionality and curiosity to the scene.

Query: Describe this photo in detail.



Base: The image depicts a painting of a cute dog dressed as an old-fashioned woman. The dog's face is adorned with **a hat and a paint mustache**, while the rest of its body features a dress. It appears to be gazing at something, perhaps exploring the painting world it's in. **Additionally, there are two more dogs in the distance, one on the left side and another towards the top right.** The scene has a blend of realistic and fantastical elements that complete the artwork.

RITUAL: The image features a painting of a dog wearing a hooded robe, giving it an artistic and mysterious appearance. The dog is positioned in the center of the painting, with its head slightly tilted to the left. The painting captures the dog's unique and intriguing look, making it the focal point of the artwork.

Figure 9. **Qualitative results on LLaVA-Bench [33].** Hallucinations are highlighted in red. RITUAL well understands ambiguous images and effectively mitigates hallucinations in outputs.



<p>Query: Is there a bottle in the image?</p> 	<p>LLaVA-1.5</p> <p>GT: No</p> <p>Base: Yes, there is a bottle visible in the image.</p> <p>RITUAL: No, there is no bottle in the image. The image shows a slice of pizza on a plate, a doll, and a person's arm.</p>	<p>Query: Is there a fire hydrant in the image?</p> 	<p>InstructBLIP</p> <p>GT: Yes</p> <p>Base: No, there are no fire hydrants in the picture.</p> <p>RITUAL: Yes, there is a fire hydrant in the image.</p>
--	---	---	--

Figure 10. **Qualitative results on POPE [28].**



<p>Query: Is there only one piece of pizza in this image? Please answer yes or no.</p> 	<p>LLaVA-1.5</p> <p>GT: No</p> <p>Base: Yes</p> <p>RITUAL: No</p>	<p>Query: Are there a white dish in the image? Please answer yes or no.</p> 	<p>InstructBLIP</p> <p>GT: Yes</p> <p>Base: No</p> <p>RITUAL: Yes</p>
---	---	---	---

Figure 11. **Qualitative results on MME [13].**

Query: Please describe this image in details.



LLaVA-1.5

Base:

The image depicts a large white moving truck, presumably carrying a delivery of brown bottles, as it either stops or drives down a road. The truck takes up a significant part of the scene, covering more than half of the image. It is parked near the side of a building, with ...

 **RITUAL:**

The image features a white truck parked on a street, with a large advertisement for beer displayed on the back of the truck. The truck is positioned near a tree, and there is another truck visible in the background. The advertisement on the truck showcases a variety ...

Query: Please describe this image in details.



InstructBLIP

Base:

The image displays a busy stage at a restaurant or food preparation facility with several chefs or cooks preparing meals. There are nine people present in the room. In addition to the cooks, there is a person observing the work from behind a fence, likely assessing the progress of the ...

 **RITUAL:**

The image features a kitchen with a man preparing food in a professional setting. He is standing in front of a counter with a large food processor, which is positioned towards the left side of the scene. The man is wearing a chef's hat and is focused on preparing the food. There ...

Figure 12. Qualitative results on CHAIR [41].

Query: How many uncut fruits are in the image?



Base:
There are **four** uncut fruits in the image.

 **RITUAL:**
There are **three** uncut fruits in the image.

Query: How many coffee mugs are in the set?



Base:
There are **four** coffee mugs in the set.

 **RITUAL:**
There are **three** coffee mugs in the set.

Query: This is the logo of LLaVA, Large Language and Vision Assistant, based on the LLaMA architecture. Please explain this logo in detail, and how do you think of its design.



Base:
Sure, I'd be happy to explain the concept and design behind the LLaVA logo. Based on the image, the LLaVA logo features a **fire-breathing** red flaming **luchador**, which may represent a mix of courage, creative expression, and energy.

 **RITUAL:**
The LLaVA logo features a unique design, combining the shape of a horse with the flames of a fire. The horse is depicted in a red color, while the flames are shown in orange. The combination of these two elements creates an eye-catching and memorable visual representation of the brand.

Query: Can you explain this meme in detail?

Sometimes I just look at pictures of the earth from space and I marvel at how beautiful it all is.



Base:
This meme is a **composite image** featuring a fried-chicken centerpiece sitting on a pan, with the shape of the dish taking the form of a map. The large piece of fried chicken consists of various pieces, distributed all over the image. A quote, presumably from Garfield, is included at the top of the image, stating, **"The earth is just spinning by and I'm frying chicken at home.** How beautiful it all is." This amusing combination of elements defines a unique and intriguing aspect of food presentation in a visually appealing manner.

 **RITUAL:**
The image features a tray of fried chicken pieces arranged to resemble a map of the world. The chicken pieces are spread across the tray, with some pieces placed near the edges and others in the center. The chicken pieces are shaped like continents and countries, creating a unique and creative representation of the world.

Figure 13. Qualitative results on LLaVA-Bench [33]. Hallucinations are highlighted in red.